Supplemental Information for

Network balance *via* CRY signalling controls the Arabidopsis circadian clock over ambient temperatures

Peter D. Gould[1^], Nicolas Ugarte[1^], Mirela Domijan[2^], Maria Costa[2], Julia Foreman[3], Dana MacGregor[5], Ken Rose[3], Jayne Griffiths[3], Andrew J. Millar[3, 4], Bärbel Finkenstädt[2], Steven Penfield[5], David A. Rand[2], Karen J. Halliday[3, 4], Anthony J.W. Hall[1]

Running title: Temperature compensation by cryptochromes

[1]Institute of Integrative Biology, University of Liverpool, Crown Street, Liverpool L69 7ZB, UK.

[2]Warwick Systems Biology and Mathematics Institute, Coventry House, University of Warwick, Coventry CV4 7AL, UK.

[3] SynthSys, C.H. Waddington Building, King's Buildings, Edinburgh EH9 3JD, UK

[4] School of Biological Sciences, University of Edinburgh, King's Buildings, Edinburgh EH9 3JH, UK

[5] School of Life Sciences, Geoffrey Pope Building, University of Exeter, Stocker Road, Exeter, EX4 4QD, UK

[^]These authors contributed equally to this work.

Table of Contents:

Supplemental Methods

Analyzing Sources of Variation using Mixed-Effects Models

Mixed-effects models (Pinheiro and Bates, 2000) are a flexible and powerful tool to describe the relationship between a response variable and a set of covariates in data that are grouped according to one or more classification factors. Mixed-effects models incorporate both fixed effects, which are parameters associated with factors (or covariates) for which the recorded levels are of specific interest, and random effects, which are associated with factors for which the levels were drawn at random from a larger population of possible levels.

The most common mixed-effects model assumes a linear relationship between the response variable and the set of covariates of interest. In this paper we followed this approach. More complex models could have been used, for example a multi-level model with several layers of hierarchy. However, for the purposes of our analysis, we felt that a linear model provided a parsimonious description with results that are coherent with the observed data.

In our data set the response variable was the estimated period length. Our covariates of interest were *light*, with levels RL, BL and R/BL, *genotype* (with levels Col-0, *cry1 cry2,phyA , phyB, cry1* and *cry2)*, *marker* (with levels *CCR2* and *CAB2)*, *temperature* (with levels 12^{o}C, 17^{o}C and 27^{o}C), *experimental replicates*, and *experimental lines*. Both *experimental replicates*, and *experimental lines* were taken to be random effects, while all other covariates were treated as fixed effects. Moreover, we treated *experimental lines* as being nested within the factor *genotype*. All fixed effects were assumed crossed in a factorial setting, while the random effect *experimental replicates* were modelled as a random intercept, allowing for differences in the overall mean period length due to variability across the replicates.

All covariates in the data were treated as categorical factors. Hence we needed to define reference levels against which all other levels for that specific factor were compared. These were R/BL for *light*, Col-0 for *genotype* (geno in model output), *CAB2* for *marker* and 12^{o}C for *temperature* (temp in model output).

We started by fitting a full model allowing for a 4-way interaction among all the fixed effects. We used the function *lmer* in the package lme4 (Bates and Maechler, 2011), implemented in the open source statistical programming environment R (R Development Core Team**,** 2011). As well as information on the period length, we also have information on

the error of the latter. We incorporate this in the model by setting the option 'weights' in *lmer* to 1/error. The results can be found in Supplementary Table 1. As the function *lmer* does not produce p-values we use, as a rough indication of significance, t-values that are greater than two in absolute value. Most of the significant interactions happen at high temperatures. In particular, the largest interaction occurs between RL and temperature at 27°C, which is not surprising given the plots in Figure 1, which show a clear increase in mean period length for RL at 27°C, consistent with the positive estimate for the effect of RL:27°C, thus completely differing from the behaviour of the reference level R/BL light. The variance estimates for both *experimental replicates*, and *experimental lines* obtained with *lmer* using restricted maximum likelihood estimation were very close to zero and substantially lower than the estimate obtained for the residual variance. Hence we can conclude that there is not significant variability across *experimental replicates* nor across *experimental lines*. We plotted the fixed effects in Figure 1D, Supplementary Figures 1B, 2B and 3B.

We also analysed the data for each light regime separately. Due to the lack of variability in the random effects we use the function *lm* in R for fitting simple linear regression models with fixed effects. The results for both BL and RL data can be found in Supplementary Table 1 and Table 2 respectively. The two light regimes seem to provide different insights into the behavior of the clock at different temperatures. While *CCR2* seems to interact with both genotype and temperature for RL data, the same is not true for BL data, where although *CCR2* has a significant lengthening effect compared to the baseline *CAB2* level, it does not interact with either of the remaining factors. Moreover, for the RL data, there seems to be a significant interaction between the marker *CCR2* and high temperature. For the BL data, the *cry1* single mutant has a significant interaction with temperature at 27°C. For the RL data this is only valid for the *CCR2* marker, suggesting a functional difference between the cells expressing the two reporter genes.

Protein Analysis

For CRY protein analysis (Supplementary Figure 5), HEPES extraction buffer 1 (100 mM HEPES, 20 mM $MgCl_2$, 1 mM EDTA, 0.10% Triton, 20% Glycerol, 2 mM DTT, with final pH of 8.0 with HCl and 10 µl per ml of Protein Inhibitor Cocktail) was added to the frozen tissue along with approximately 0.5% polyvinylpyrrolidone (PVPP) and a titanium ball. The samples were ground and centrifuged for 5 min at 4°C. The supernatant was removed to a new tube and centrifuged again. This clarified supernatant was again transferred to a new

tube. Protein concentration was determined using Bradford reagent (Sigma cat# B6916) standardized against bovine serum albumin (BSA) (10mg/ml from NEB cat# B9001S). Equal volumes of protein were loaded onto pre-cast RunBlue SDS Gel 4-12% (17-wells Expedeon cat# NXG41227). The gels were run according to the manufacturer's guidelines (180 Volts, 180 Amps, for ~45 minutes). Protein transfer was accomplished using Invitrogen's iBlot protocol. Once transferred, the membrane was stained with Ponceau S solution (0.1% (w/v) Ponceau S in 5% (v/v) acetic acid) as a loading control and blocked overnight in 5% Marvel TBST. Detection was accomplished using Millipore's SNAP ID Western Blotting Protein Detection System. The primary antibodies used were anti-CRY1 at 1:5000 dilutions and anti-CRY2 at 1:2500 dilutions. Use of these antibodies had previous been described in (Zeugner et al., 2005). The secondary antibody used was Goat Anti-Rabbit IgG - HRP (Insight Biotechnology SC-2004) at a 1:5000 dilution. Enhanced chemiluminescence (ECL) quantitation was done with Millipore's Immobilon HRP chemiluminescent substrate (Fisher Scientific cat# MDR-100-020T). Detection of protein was accomplished using G-BOX iChemi chemical imager (Syngene) and GeneSnap image acquisition software. In Photoshop integrated band density was calculated. To normalize across several membranes, standard samples were loaded of known protein concentrations allowing the production of a standard curve from which levels of CRY1 and CRY2 were calculated. Finally, CRY protein levels were normalized by the amount of protein loaded to give relative CRY concentration per total protein.

For LHY protein analysis (Figure 3), two ⅛ inch balls (Spheric Trafalgar Ltd) were added to the frozen tissue samples and the plant material ground using a MM300 TissueLyser (Retsch) using pre-cooled tube adapters. Protein extraction buffer described in Devlin *et al*., 1992 (excluding individual protein inhibitors, but including complete EDTA-free protease inhibitor cocktail (Roche) and 1mM DTT) was added to each sample, 100µl/100 µg material. Following centrifugation, the soluble protein lysate was collected and 21µl was run on a 10% gel, followed by a wet transfer to PVDF membrane following standard laboratory procedures. The LHY protein was detected using a native LHY antibody (Kim *et al*., 2003) at dilution 1:500 followed by a HRP-conjugated goat anti-rabbit antibody (Biorad cat#172-1019) at a dilution of 1:3000. Blots were reprobed with anti-RPN10 antibody (Abcam cat#ab60101, anti-26S proteosome regulatory subunit antibody (At4g38630)) at dilution 1:5000 as a loading control, followed by a HRP-conjugated goat anti-rabbit antibody as above. Signals were detected using the Amersham ECL kit (GE Healthcare cat#RPN2106) as per

manufacturer's instructions. Individual bands on blots were quantified using Metamorph (Molecular Devices) integrated intensity method. Loading was normalised using the RPN10 band (LHY band intensity / RPN10 band intensity). A reference sample (Ref, in figure) (containing moderately high levels of LHY protein) was loaded onto each blot to allow normalisation between blots. The normalised LHY protein level in the reference sample was set to 1 and LHY protein levels in experimental samples were expressed as a ratio of this reference sample. The experiment was carried out in biological triplicate and the mean LHY protein levels and SE were calculated for each time point.

Temperature-dependence of biochemical reactions, and consequences for the circadian clock

Simple biochemical reactions typically obey van't Hoff's rule, which suggests that the change in their reaction rate for a 10°C temperature rise (Q_{10}) is roughly double or triple (Q_{10}=2-3). This "rule" is a particular case of the empirical, Arrhenius relation, where a reaction rate *r* takes the form.

$$r = A_j e^{\frac{E_j}{RT}} \qquad (1)$$

R represents the universal gas constant (8.3145 x 10^{-3} kJ mol^{-1} K^{-1}), T represents temperature (in Kelvin). E_j is the particular reaction's activation energy. A_j is a reaction-specific constant, termed the Arrhenius constant or collision factor, which has no effect on the relative change in rate with increasing temperature. When T is close to ambient and *E* is in a typical range of biochemical reactions (40-50 kJ mol^{-1}), *r* roughly doubles for a 10K increase in T, yielding van't Hoff's rule.

The period of the circadian clock typically shows Q_{10} = 1.0 to 1.4 (Dunlap et al., 2003) over a 15-20K temperature range. Temperature compensation was defined as near-invariance of period over a temperature range. Indeed, $Q_{10} \approx 1.0$ was observed in some canonical experimental species (Pittendrigh, 1954). A controlled change of period with temperature is more commonly observed, however, suggesting that a specific change in period might be advantageous (Akman et al., 2008). Hence we discuss mechanisms for period control, rather than temperature compensation in the sense of $Q_{10} \approx 1.0$.

Circadian period control is remarkable, because this property is rare among chemical oscillators, though it is not unknown (Rabai and Hanazaki, 1999). In contrast, biochemically realistic mathematical models of circadian circuits do not necessarily remain rhythmic when many key rate parameters are doubled. Indeed few such models do so unless temperature

compensation has been explicitly incorporated (Akman et al., 2008). Thus the most surprising feature of temperature compensation might not be the small change in period, but rather the fact that the clock remains rhythmic at all over a wide temperature range. This observation is so widespread across experimental systems, however, that it is taken for granted. From this alternative perspective, the control of period might seem comparatively easy, given a clock system that achieves the harder feat of retaining rhythmicity over a wide temperature range.

More remarkably still, all circadian clocks can be reliably synchronised by daily temperature cycles (Dunlap et al., 2003). Thus the circadian system must combine a well-defined sensitivity to temperature changes, with robustness to a range of constant temperatures.

Modelling the temperature-dependence of light input to the clock

The earlier, two-loop model (Locke et al., 2005) had suggested that the morning and evening loops contributed differentially to temperature compensation (Gould et al., 2006) but did not address the role of light inputs. Simulation of an earlier, two-loop clock model showed that lower LHY transcription, representing 27C and tending to shorten period, could be balanced by higher transcription of the hypothetical evening loop component *Y* (representing *GI*), to control the period in the wild type. Transcript levels in this model were otherwise unconstrained, but rhythmic amplitude was shown to be sensitive to simulated mutation of *Y* (Gould et al., 2006) The period control coefficients of *LHY/CCA1* and *GI* transcription have opposite sign in the current model (Supplementary Table 3), indicating that a similar balance could in principle be established by these parameters, in the absence of other constraints. However, *GI* and other transcript levels would change substantially with temperature, in contradiction to our present data.

Our analysis started from the more recently developed Pokhilko et al. (2010) that comprises a morning loop with the components LHY/CCA1 and PRR9, PRR7 and NI (Night Inhibitor, a potential PRR5 candidate), and the evening loop comprising TOC1 and Y, GI and ZTL. The model also includes a pair of negative feedback loops connecting the morning and evening loop components, TOC1 and LHY/CCA1, via the protein called TOC1 modified (a proxy for gene X from the Locke et al. (2006) model and also through negative feedback of TOC1 on PRR9.

The model consists of 19 non-linear differential equations, representing the mRNA and

protein levels of the genes LHY/CCA1, TOC1, PRR9, PRR7, NI, Y and GI, as well as proteins of ZTL, modified LHY modified TOC1 and the ZTL-GI (ZG) complex. Light enters the model from two sources: (i) a light function θ (where lights-on is modeled as theta=1 and lights-off as θ=0) and (ii) a protein P which degrades in the light and accumulates in the dark. Light affects the transcription of components LHY/CCA1, Y and GI through both these mechanisms and the transcription of PRR9 via P only. Light also effects translation of LHY, GI-ZTL complex formation, and protein degradation of TOC1, PRRs and NI as well as degradation of TOC1 modified, solely through light (θ) function. In continuous light, protein P is quickly degraded to zero, so the only light input is via the on/off light function theta. Hence, in the continuous light conditions used in our temperature studies, the Pokhilko model has eleven light-dependent parameters, from aforementioned sources (for exact values please refer to Supplementary Table 3).

Our experimental data indicated that light signalling was required to maintain circadian period across temperatures. We therefore set out to test whether the light regulated inputs to the clock were required for temperature compensation, by assigning temperature sensitivity to each of the light-dependent parameters.

Our list of modeling constraints ranked in order of decreasing importance is:

1. Period profile in WT plants at 12°C, 17°C and 27°C. Relative levels of clock gene mRNA in WT plants across 12°C, 17°C and 27°C (more precisely, *PRR9* mRNA level triples from 12°C to 27°C, *TOC1* level doubles, and all other mRNA levels stay constant across all three temperatures). Phase differences among clock gene rhythms in WT plants at each temperature (Figure 2).

2. Period profile in *cry1cry2* mutants. Low mRNA levels of LHY and PRR9 in the *cry1cry2* double mutant at each temperature compared to WT mRNA levels. High mRNA level of GI in the *cry1cry2* double mutant at each temperature compared to WT mRNA levels. mRNA levels of TOC1 must be similar to mean WT levels.

3. Period profile in *cry1* single mutants.

Temperature compensation of the WT model

We assumed that temperature compensation may be achieved by the balance of opposite

reactions, as hypothesized by Hastings and Sweeney (1957). Following the work of Ruoff (1992; 1994; Ruoff et al., 2000), we consider that the dependence of the rate constants of the chemical reactions on temperature is described via the Arrhenius equation (1). Temperature compensation means that the slope of the period change with respect to temperature, dp/dT, remains close to zero, dp/dT≈0. The period slope with respect to temperature can be written in terms of activation energies E_j and control coefficients c_j where

$$\frac{dp}{dT} = (p/RT^2)(c_1E_1 + c_2E_2 + ... + c_mE_m). \quad (2)$$

The mathematical expression of each sensitivity coefficient takes the form $c_j = \partial \log p / \partial \log k_j$. Each term $(p/RT^2)c_jE_j$ corresponds to the sensitivity of period to changes in temperature, as mediated by the parameter k_j.

In order to achieve temperature compensation, we followed the global temperature compensation method preformed in (Akman et al., 2008), where all temperature-sensitive parameters are balanced at two temperatures (T1=12°C and T2=27°C) so that dp(T1)/dT≈0 and dp(T2)/dT ≈0.

In general, a model can temperature compensate if the period sensitivity coefficients of two parameters are of opposite sign at both temperature extremes, because this offers the possibility of balancing Ruoff's expression.

Our original 27°C model took all its parameter values from the Pokhilko et al. 2010 model (modeled on 22°C white light experimental data), because this model has a free-running period of 24.5h, matching the period profile of the BL model at 27°C. The parameters from the WT model at 12°C were determined by decreasing the values of the 27°C model and trying to match the period at 12°C. We found that at both temperature extremes (12°C and 27°C) there were parameters with sensitivity coefficients of opposite signs. Moreover, all these parameters preserved their signs, independently of temperature level (Supplementary Table 3). Parameters with positive coefficients were identified as the following: LHY transcription (n0), translation (p1), Y transcription (n5) and PRR9 protein degradation (m13). These parameters lead to period lengthening with increasing temperatures. On the other hand, parameters with negative coefficients were identified as: degradation of LHY (m1), TOC1

(m6), TOC1 modified (m25), PRR7 (m15), NI (m17), transcription of GI (n12) and formation of ZG complex (p12). This latter set of parameters has an opposite effect and leads to period shortening with increasing temperature.

Since there are parameters with opposite sensitivity coefficients at both temperature extremes (12ºC and 27ºC), with just a handful of the parameters (those with largest coefficients) we could reproduce the period profiles and model the time-series at both temperature extremes (Supplementary Figure 6, Supplementary Table 3). Our selection criteria is that the parameter has to have at least one sensitivity coefficient above 20% of the largest sensitivity coefficient at all temperatures (LHY mRNA degradation at 27ºC). The parameters used in temperature compensation of the WT are: LHY transcription (n0), mRNA degradation (m1), translation (p1), TOC1 protein and TOC1modified protein degradation (m6 and m25, resp.), PRR7 degradation (m17) and GI transcription (n12). Our WT model can temperature compensate (Supplementary Table 3) and it gives a good match to the RNA time series (Figure 2) and a good match to the experimental WT period profile (Figure 1).

The model circuit can match *cry1* single mutant data

Our WT model provided a good starting point for identifying parameters of the *cry1* single mutant model, since period profiles of the WT and cry1 mutant at 12ºC are almost identical, and they are within 2h difference at 17ºC and 27ºC (Figure 1).

We assumed that the *cry1* mutant would have an effect on the light-dependent interactions, leaving much less light-activated transcription and light-accelerated degradation than in the WT, but increasing the rate of degradation that is usually decelerated with light. In the Pokhilko et al. 2010 model, degradation of PRR9, PRR7, NI and TOC1 is accelerated in the dark, hence, in order to model the *cry1* mutant, these parameters should have higher (or equal) values than the WT model. All other light parameters should have lower (or equal) values than the WT model. This constraint is added to our manipulation of only light-responsive parameters, and to the Arrhenius form of their temperature-dependence.

Since WT and cry1 mutant period profile at 12ºC is similar (Figure 1), we let cry1 mutant parameters be identical to WT model parameters at 12ºC. To model the cry1 mutant at higher temperatures, we started with the counterpart WT models, and we used the information on the parameter sensitivities of WT models to first identify a single parameter

which could be modified from its WT value in order to match the period profiles observed (Figure 1). We identified degradation of PRR9 protein (parameter m13) as a potential candidate, since increasing this parameter from the WT model value at 17ºC and 27ºC increases the period. We found that increasing the value of this parameter at 17ºC and 27ºC from its WT counterpart was sufficient to match the cry1 single mutant period profiles,

Our model of the *cry1* mutant could match the period profiles, maintaining a longer period than the WT at 27ºC (Supplementary Figure 6).

The model circuit matches the *cry1 cry2* double mutant data only by relaxing one constraint.

The data of the *cry1 cry2* double mutant shows that the clock rapidly damps to arrhythmia at the high temperature of 27°C, and has a longer period at 12°C and 17°C. We hypothesized that the effect of the *cry1 cry2* double mutant under BL would be more severe than the effect of *cry1* mutant, leaving much less light-activated transcription and light-accelerated degradation than in the WT, but further increasing the rate of protein degradation that is deccelerated with light. In the Pokhilko et al. 2010 model, degradation of PRR9, PRR7, NI and TOC1 is accelerated in the dark, hence, in order to model the *cry1 cry2* mutant, these parameters should have higher values than the WT and *cry1* mutant model. All other light parameters should have lower values than the WTand the *cry1* mutant models. This constraint is added to our manipulation of only light-responsive parameters, and to the Arrhenius form of their temperature-dependence.

It was already known that arrhythmia cannot be achieved by reducing transcription or translation of *LHY/CCA1* alone, namely by lowering parameters n0 and p1, because the models were designed to simulate the remaining, short-period rhythms in the *lhy cca1* double mutant (Locke et al., 2005; 2006). We also tested decreasing the other parameters (or increasing in the case of parameters of PRR9, PRR7, NI and TOC1 degradation) that were identified as light parameters and as temperature sensitive in the WT (Supplementary Table 3), but none of the models tested had arrhythmic behaviour (unpublished results). Thus the *cry* mutants must affect some combination of genes represented by at least several of the light-activated components in the model.

Our first attempt was to change values of the temperature-sensitive parameters of the WT

model (Supplementary Table 3) at both 12°C and 27°C to calculate the *cry1 cry2* mutant model values. We found that no matter which parameter combinations we tried, we could not change parameter values of the WT model at 27ºC to obtain arrhythmic behaviour. However, we had more success when we matched the *cry1 cry2* mutant data at 12ºC and then tried to increase the parameter values to get the arrhythmic behaviour at 27ºC (Supplementary Table 4).

This model of the *cry1 cry2* double mutant showed the loss of rhythmicity at 27ºC, and showed a good match in period profile at low temperature (28.36h at 12ºC), but predicted a lower period at 17ºC than observed (25.1h at 17ºC) (Supplementary Figure 6). PRR9 (at higher temperatures) and TOC1 genes relative mRNA levels matched the experimental data for the double mutant compared to the WT (Figure 2). For *GI* mRNA, the *cry1 cry2* double mutant levels were consistently too low compared to the data, which could reflect the limited constraints available during the construction of the original Pokhilko 2010 model, as discussed (Pokhilko et al, 2010).

For *LHY* mRNA, the *cry1 cry2* double mutant levels were consistently too high compared to the data. Despite this, the model could correctly predict the low levels of LHY protein observed in the data. The *cry1 cry2* double mutant has lower levels of LHY translation, but this is not the cause of the low protein levels. We test how much effect translation has on the levels of LHY total protein by increasing the level of LHY translation from the mutant value (p1=0.19) to the original WT value (p1=0.4) while not changing any of the other *cry1 cry2* mutant parameters. We found that the levels of LHY total protein do increase as p1 is increased, but they are still significantly lower that the corresponding WT levels, An increase in translation parameter (p1) has a negative feedback effect on the LHY mRNA levels (via increasing the PRRs), and hence there is a trade-off in translation of a higher translation constant (p1) and lower LHY mRNA levels. Hence, the relative difference in LHY proteins levels in the mutant vs.WT is not caused by a change in the translation rate (p1). Rather, it is a result of a more complex feedback. Though high levels of mRNA (with translation parameter unchanged) will lead to higher protein levels, this is an overly simplistic view of LHY dynamics, since LHY protein has a negative feedback on mRNA levels.

Thus, with these possible exceptions, the model circuit proved sufficient to match both the period profiles and the RNA time-series data.

Finally, we tested whether the model parameters are close to a Hopf bifurcation. In case of our models, being close to a Hopf bifurcation, means that by introducing small changes in some parameters one can change the dampened oscillations to sustained oscillations, or vice versa. In our models with dampened oscillations, these dampened oscillations eventually converge to a steady state. In models with sustained oscillations there is also a steady state, but it is not visible in simulations since it is repelling any initial conditions starting close to it (this is called an unstable steady state). To detect whether the models are close to a Hopf bifurcation we need to look at a set of, so-called, eigenvalues that are associated to each steady state. A model of n variables will have n eigenvalues associated to a steady-state. In a model of 19 variables there will be 19 eigenvalues associated to each steady state. Eigenvalues can be real numbers, or come in pairs, as a pair of complex numbers. As the model parameters are changed, the steady state will change and so will its eigenvalues. If the model undergoes a Hopf bifurcation, then there exists a pair of complex eigenvalues whose real part will go through the 0 value as parameters are changed. Similarly, a model is close to a Hopf bifurcation if it has a pair of eignevalues with real part close to 0.

At all three temperatures the *cry1 cry2* double mutant model is close to a Hopf bifurcation.

At 12ºC, *cry1 cry2* mutant model has stable oscillations that after some time settle to a rhythm of 26.15h. Aside from these oscillations, the model also has an unstable steady state. All eigenvalues of this steady state have negative real parts, except for one pair. This pair of complex eigenvalues, 0.006874 + i *0.249063 and 0.006874- i *0.249063, have real parts positive and close to 0.

At 17ºC, *cry1 cry2* mutant model has damped oscillations, and the model reaches a steady state approximately 300h after transfer to constant light conditions. This model contains a stable steady state that has two pairs of eigenvalues with negative real part close to 0. These eigenvalues are (-0.01+i*0.26 and-0.01-i*0.26, and, -0.06 -i*0.31 and -0.06 +i*0.31.

At 27ºC the *cry1 cry2* mutant model has a stable steady state with two pairs of eigenvalues with real parts close to 0. These eigenvalues are -0.06 +i*0.37 and -0.06-i*0.37, and -0.05+i*0.25 and -0.05-i*0.25.

With the models that are close to a Hopf bifurcation, it is also possible to give predictions of the average period of the oscillations that one can expect to see. In theory, if parameters are

chosen so that the model is sufficiently close to a Hopf bifurcation, the limit cycle solutions (that surround the steady state should have period close to ($2\pi/\omega$), where ω is the imaginary part of the pair of eigenvalues that cross the real axis. In the *cry1cry2* mutant model, one would expect to see long-term rhythms (either sustained or decaying) ranging between 24h to 25h across all three temperatures (more specifically, 25.2h ($2\pi/0.249063$) at 12ºC, 24.17h ($2\pi/0.26$) at 17ºC and 25.13h ($2\pi/0.25$) at 27ºC).

Comparison to analysis of the Pokhilko et al. (2012) model

mRNA profiles of PRR9 (at 12ºC), GI and LHY (at all three temperatures) of the *cry1 cry2* mutant model are not a close fit to the data (Figure 2). In order to check whether we can improve the fit by switching to a more recent underlying model structure, we consider the comparison of the models of the Pokhilko et al. (2010) and Pokhilko et al. (2012). These are henceforth referred to as the 2010 model and the 2012 model. The latter comprises a morning loop with components LHY/CCA1 and PRR9, PRR7 and NI (Night Inhibitor, a potential PRR5 candidate), and an evening loop comprising TOC1, GI, LUX, ELF3, ELF4, EC (evening complex, an actual complex of ELF3, ELF4 and LUX) and COP1. There are structural differences between the two models. Aside from the addition of the evening components LUX, ELF3, ELF4 and EC (and their connections), several of original connections between morning and evening loops are modified in the 2012 model: feedback to LHY from TOC1 is now negative; EC has negative feedback on LHY; the negative feedback of evening loop on PRR9 now comes through EC (not TOC1, as is the case in the 2010 model); and GI now is inhibited by EC instead of TOC1.

The 2012 model consists of 28 non-linear differential equations, representing the mRNA and protein levels of the genes LHY/CCA1, TOC1, PRR9, PRR7, NI, LUX, ELF4, as well as proteins of ZTL, LHY modified protein, mRNA of ELF3 and GI, cytoplasmic proteins of ELF3, GI, COP1, and nuclear proteins of ELF3, GI and COP1 in day and night forms, and the cytoplasmic protein complexes ELF3-GI, GI-ZTL (ZG) and nuclear protein complexes ElF3-GI, ELF3-ELF4, EC.

Light in the 2012 model enters through same two sources (protein P and direct light input) as in the 2010 model. Pokhilko et al, (2012) has ten light-dependent parameters. Parameters retained from the 2010 model are LHY mRNA degradation, LHY translation, protein

degradation of PRR9, PRR7, NI, TOC1 and ZTL-GI complex formation. The model also additionally has light parameters for EC degradation, COP1 cytoplasmic and night-active form protein degradation (modeled as a single parameter), and COP1 day-active form protein degradation (for exact values please refer to Supplementary Table 6).

Matching *cry1 cry2* double mutant in the Pokhilko et al, (2012) model.

We choose the parameter values of the 2012 model (modeled on 22°C white light experimental data) as parameters values for the WT 27°C model in blue light, since the WT 27°C BL model has the same constant light period of oscillations as the 2012 model. In order to test whether the switch from the 2010 model to the 2012 model improves the fit to the *cry1cry2* double mutant data, we will first try to fit the model to data at 27°C. As in the earlier modeling of photoreceptors, this implies several restrictions on changes that can be made to light parameters.

First, we investigate the effect of the change of TOC1 feedback on LHY from positive in the 2010 model to negative in the 2012 model). Since both models were made under the constraint that the *toc1* mutant has shorter period, we expect that any changes to light parameters associated with TOC1 will have the same effect on period in both models. As expected, we find the sign for the sensitivity coefficient of TOC1-dependent light parameter is the same in both models (Supplementary Table 6 for the 2012 model) . In both models the sensitivity coefficient is negative, and hence increasing TOC1 protein degradation decreases period of oscillations. Hence in both models, TOC1 plays the same role in temperature compensation based on period profiles.

Aside from a light parameter linked to the evening complex EC, the 2012 model shares all other parameters with significant sensitivity coefficients with the 2010 model (Supplementary Table 6). As significant sensitivity coefficients, we include those which are greater than 10% of the largest sensitivity coefficient (LHY mRNA degradation, (m1)).

In order for the 2012 model to match the 27°C *cry1cry2* double mutant data, the following changes to the mRNA and protein profiles have to be achieved:

(i) mutant LHY mRNA and total protein levels have to decrease and match the level of the respective WT troughs;
(ii) mutant PRR9 mRNA levels have to decrease and match the level of the WT

trough;

(iii) mutant TOC1 mRNA levels have to be similar to the average WT levels; and

(iv) mutant GI mRNA levels have to be increased but stay below the peak WT level.

We can estimate the effect that changes in any parameter will have on the timeseries of a chosen mRNA or protein. The change to a timeseries of an mRNA or protein (g(t)) brought on a by a relative change to a parameter k from k_0 to k_1 can be approximated by $dg/dk(t)*(k_1 - k_0)$ using the partial derivative dg/dk.

We can calculate the partial derivatives where solutions (g) are scaled so that their period is not parameter dependent, and these partial derivatives only reflect the changes in shape of solutions (g), not changes in period. For a model with a given periodic solution (i.e. timeseries) we can calculate these partial derivatives from (Rand, 2008). In Supplementary Figure 7 we show the total change to the PRR9 mRNA over one full cycle, when each light parameter is perturbed. We have taken into account whether the parameter is only allowed to increase or decrease, as stipulated by our earlier modeling restrictions, but have not set the relative change in the parameter value. Taking into account the relative change in the parameter value will just scale the corresponding curve by that factor. For example, if we halved the value of LHY transcription (parameter, m1), we would have to multiply the corresponding curve (blue) by 0.5. This would then lead to an increase in the PRR9 mRNA peak level. On the other hand, changes to evening complex (EC) degradation (parameter p24) would lead to a decrease in the PRR9 mRNA peak level. In order to assess the effect of changes to several parameters, it is enough to sum the effects each parameter will have. The effect of each parameter on every mRNA and protein level of interest are shown in Supplementary Figures 7-11.

To check the validity of approximations, we modified each parameter in turn by 50%. We found that when all parameters (except for LHY mRNA degradation, m1 and COP1 cytoplasmic and night-active form protein degradation ,p15) are changed by this amount the model simulations match the overall changes predicted by the sensitivity analysis. LHY mRNA degradation (m1) and COP1 degradation (p15) can be lowered by at most 45% so that simulation of GI mRNA still matches the prediction that levels of GI mRNA behave like PRR9 mRNA levels.

As stated above, the 2010 model cannot match condition (i) (LHY mRNA levels are too

high) and condition (iv) (GI mRNA levels are too low). Next we outline whether these fits can be improved with the 2012 model.

Any parameter changes will have a similar effect on PRR9 mRNA and GI mRNA, hence making it impossible to match conditions (ii) and (iv) simultaneously. Overall levels of PRR9 mRNA in the mutant can be achieved by changing EC degradation (p24). This will lower the peak of PRR9 mRNA. However, a change in EC degradation also has a negative effect on GI mRNA levels (Supplementary Figure 8). In order to match the mutant, GI mRNA levels have to be increased overall, leading to a contradiction. There are no other parameters which give a strict decrease in PRR9 mRNA levels, though a possible combination might involve changing LHY translation (p1) and degradation of either PRR9, NI or TOC1 (parameters m13, m15, m6). However, these parameters also have a similar effect on GI mRNA, hence, if we lower the PRR9 mRNA levels by any of these parameter combinations, this will also lower GI mRNA levels, again leading to a contradiction.

In summary, improvement in the fit to GI mRNA mutant 27C levels in the 2012 model will come at an expense of PRR9 mRNA fit.

Now we turn to improving the fit to condition (i). Parameters p24 (EC degradation), p15 and m31 (COP1 protein degradation) have the greatest effect on lowering LHY mRNA and protein levels (condition (i)), Supplementary figures 10-11. The only other parameters that lower LHY mRNA and protein levels are m17 and p12, but they have a negligible effect. As stated above, each of these parameters has a similar effect on PRR9 and GI mRNA. So it is impossible to reconcile conditions (ii) and (iv). Moreover, these parameters also have a similar effect on TOC1 mRNA, Supplementary Figure 9. For example, parameter p24 decreases peak levels, while p15 and m31 increase peak levels. This indicates that it is not possible for all three of PRR9, TOC1 and GI to have clearly opposite behaviours (as required by conditions (ii)-(iv)). Changing all five parameters by about 50% leads LHY mRNA peak to decrease threefold, while TOC1 and PRR9 oscillate around the average WT level and GI oscillates below average WT level.

In summary, the improved fit to mutant LHY mRNA levels could be achieved with the 2012 model, but it would come at the expense of two of the three other mRNAs. The choice of which two have worse fits will depend on the parameters used.

The statements above refer to creating the *cry1cry2* 27°C mutant model starting at WT 27°C

parameter values. They are reproduced in Table 2 of the main text.

Next we try to create the 2012 WT model at 12°C. If this is possible, then we can address the question of whether the 2012 model can give a better fit to the 12°C *cry1cry2* mutant data. Moreover, we can also address the question of whether we can construct a 27°C *cry1cry2* mutant starting from 12°C *cry1cry2* mutant values. Note that in the 2010 model we also could not create the *cry1cry2* 27°C mutant model starting from WT 27°C values. Instead, for the 2010 model, we fitted 27°C mutant starting from the *cry1cry2* 12°C mutant model. The *cry1cry2* 12°C mutant parameters themselves were determined by starting from WT 12°C model parameters.

Candidate parameters for getting the correct period profile at 12°C (i.e. for increasing period) are m1, p12 and p15, Supplementary Table 6. Note that parameters like degradation of PRRs and TOC1 proteins also have negative period sensitivity coefficients, but these parameters must increase with lower temperature (due to parameter constraints described earlier), hence changing their values would have an undesired effect of decreasing the period. Changes to any of the three parameters (m1, p12, p15) always lead to an increase in PRR9 mRNA levels (Supplementary Figure 7), hence with these three parameters the model is not able to reproduce one of the most striking features of WT 12C data: that PRR9 mRNA decreases threefold with falling temperature. The only way to decrease PRR9 mRNA is to introduce temperature into other parameters, but this comes at the expense of the period profile fit. The parameters that decrease PRR9 mRNA levels such as p24 and m6, also have large period sensitivity coefficients. The only parameter that decreases PRR9 mRNA levels and has low period sensitivity coefficient is p1 (LHY translation). However, most of the effect of p1 on PRR9 mRNA levels gets canceled out by the effect of m1 (the only parameter that can significantly increase period), Supplementary Figure 7 (middle panel). With all this information, we conclude that it does not appear possible to identify a set of parameters with which we could simultaneously achieve a WT period profile at lower temperatures and also get a good fit to PRR9 mRNA levels. In fact, changing m1, p1, p15 and p12 by 50% leads to period of 26.1h, with PRR9 peak only falling by about 25%.

This leads us to conclude that a good fit of 2012 model to WT data at low temperatures cannot be achieved. This also means that we cannot follow the modeling procedure outlined for the 2010 model and we have no means of starting to construct the *cry1cry2* mutant models.

Detailed discussion of the cry mutant modelling

The success in matching the starting data and in predicting a specific, molecular phenotype suggests that the model captures significant parts of the temperature compensation mechanism in the WT plants. The difficulty in matching the arrhythmia of the double mutant arose, not from the model circuit, but from a conflict that is inherent in our assumptions. The mutant parameter values at 27°C must increase from their values at 12°C, as required by the Arrhenius temperature-sensitivity terms in the model. To comply with the mutant-effect constraint (above), the mutant parameter values should also remain lower than their counterparts in the WT at 27°C. Obviously, the WT parameter values do not lead to arrhythmia at 27°C. Thus to match the data under these constraints, we required low parameter values to give rhythms at 12°C in the double mutant, increasing some of the parameter values to abolish the rhythms to match the mutant's arrhythmia at 27°C, and increasing the parameter values further to restore the strong rhythms of the WT at 27°C. This is not impossible. It is a very severe set of constraints, however, and they discriminate among our assumptions. The present model's behaviour provides an informative example, that helps to show how the data suggest which assumptions are worth questioning.

The model lacks some known processes that might be relevant to temperature and/or light input. Including these in the model would help to understand the molecular mechanisms at work. Such an expanded model might not help to match the *cry1 cry2* double mutant data. The same Arrhenius and mutant-effect assumptions would apply to any new parameters in an extended model (and to existing, non-light-dependent parameters), leaving the severe constraints intact.

In contrast, the cry proteins are not explicitly modelled. Though the mutations definitely reduce cry function, they might indirectly increase a parameter value in the model, even if it is light-activated, violating the mutant-effect assumption. Alternatively, the Arrhenius relationship derives from elementary chemical reactions, so a more complex macromolecular process might reduce its rate with increasing temperature, at least above some optimum temperature. The Arrhenius and mutant-effect assumptions may hold for many of the relevant processes, but experiments to test their generality seem well justified.

Modelling the *prr7/9* mutant and the *cca1/lhy* double mutant.

In order to model the *prr7/9* mutant, the translation rates of PRR7, p8, and PRR9, p9, were set to 0.01, while other parameters kept their WT model values. The *prr7/9* mutant at 17°C and 27°C can entrain to 12L:12D cycles, while at 12°C the mutant shows quasiperiodic behaviour. The period of the *prr7/9* mutant increases with temperature (23.5h at 12°C, 22h at 17°C and 25.5h at 27°C), as described (Salome et al., 2010).

To model the *cca1/lhy* double mutant the translation rates of LHY/CCA1 in light, p1, and dark, p2, are set to 0. The *cca1/lhy* mutant at all three temperatures can entrain to 12L:12D cycles. The *cca1/lhy* double mutant model has a lower period than the WT at all three temperatures (Supplementary Figure 13B), consistent with experimental observations (Supplementary Figure 13D).

The P2010 model is accessible from the Biomodels database in a variety of formats, accession number BIOMD0000000273 - Pokhilko2010_CircClock, and from the PlaSMo repository (www.plasmo.ed.ac.uk), accession PLM_6. The models presented here will be available from the same locations upon publication.

Supplemental References

Akman, O.E., Locke, J.C.W., Tang, S., Carré, I., Millar, A.J., and Rand, D.A. (2008). Isoform switching facilitates period control in the *Neurospora crassa* circadian clock. *Mol Syst Biol* **4**: 164.

Bates, D. M. and Maechler, M. (2011). lme4: Linear mixed-effects models using S4 classes. R package version 0.999375-37/r1160.

Czechowski T, Bari RP, Stitt M, Scheible W-R & Udvardi MK (2004) Real-time RT-PCR profiling of over 1400 Arabidopsis transcription factors: unprecedented sensitivity reveals novel root- and shoot-specific genes. *Plant J* **38:** 366–379.

Devlin, P.F., Rood, S.B., Somers, D.E., Quail, P.H., Whitelam GC. (1992) Photophysiology of the Elongated Internode (*ein*) Mutant of Brassica rapa: ein Mutant Lacks a Detectable Phytochrome B-Like Polypeptide. *Plant Physiol.* **100**: 1442-7.

Dunlap, J.C., Loros, J.J., DeCoursey, P.J. (2003). Chronobiology: Biological Timekeeping. (Sinauer Associates Inc, Sunderland, USA).

Edwards, K.D., Lynn, J.R., Gyula, P., Nagy, F., and Millar, A.J. (2005). Natural allelic variation in the temperature-compensation mechanisms of the Arabidopsis thaliana circadian clock. *Genetics* **170:** 387-400.

Gould, P.D., Locke, J.C., Larue, C., Southern, M.M., Davis, S.J., Hanano, S., Moyle, R., Milich, R., Putterill, J., Millar, A.J., and Hall, A. (2006). The molecular basis of temperature compensation in the Arabidopsis circadian clock. *Plant Cell* **18,** 1177-1187.

Gould, P.D., Diaz, P., Hogben, C., Kusakina, J., Salem, R., Hartwell, J., and Hall, A. (2009). Delayed fluorescence as a universal tool for the measurement of circadian rhythms in higher plants. *Plant J* **58**: 893-901.

Hall A, Bastow RM, Davis SJ, Hanano S, McWatters HG, Hibberd V, Doyle MR, Sung S, Halliday KJ, Amasino RM & Millar AJ (2003) The TIME FOR COFFEE gene maintains the amplitude and timing of Arabidopsis circadian clocks. *Plant Cell* **15**: 2719–2729.

Hastings, J.W., and Sweeney, B.M. (1957). On the Mechanism of Temperature Independence in a Biological Clock. *Proc Natl Acad Sci USA* **43:** 804-811.

Kim, J., Song H., Taylor B. L., Carre I.A. (2003) Light-regulated translation mediates gated induction of the Arabidopsis clock protein LHY. *The EMBO Journal* **22**: 935-944.

Locke, J.C.W., Southern, M.M., Kozma-Bognar, L., Hibberd, V., Brown, P.E., Turner, M.S., Millar, A.J. (2005) Extension of a genetic network model by iterative experimentation and mathematical analysis. *Mol Syst Biol* **1**: 13.

Locke, J.C., Kozma-Bognar, L., Gould, P.D., Feher, B., Kevei, E., Nagy, F., Turner, M.S., Hall, A., and Millar, A.J. (2006). Experimental validation of a predicted feedback loop in the multi-oscillator clock of *Arabidopsis thaliana*. *Mol Syst Biol* **2:** 59.

Marshall, O.J. (2004). PerlPrimer: cross-platform, graphical primer design for standard, bisulphite and real-time PCR. *Bioinformatics* **20**: 2471-2472.

Pinheiro, J. C. and Bates, D. M. (2000). *Mixed-Effects Models in S and S-plus*. Springer.

Pittendrigh, C.S. (1954) On temperature independence in the clock system controlling emergence time in Drosophila. *Proc Natl Acad Sci U S A* **40**: 1018-1029.

Pokhilko, A., Hodge, S.K., Stratford, K., Knox, K., Edwards, K.D., Thomson, A.W., Mizuno, T. & Millar, A.J. (2010) Data assimilation constrains new connections and components in a complex, eukaryotic circadian clock model. *Mol Syst Biol* m**6:** –

Pokhilko, A., Fernández, A. P., Edwards, K. D., Southern, M. M., Halliday, K. J., & Millar, A. J. (2012). The clock gene circuit in Arabidopsis includes a repressilator with additional feedback loops. *Mol Syst Biol*, **8**: 574.

Rabai G & Hanazaki I (1999) Temperature compensation in the oscillatory hydrogen peroxide-thiosulfate-sulfite flow system. *Chem Commun* 1965–1966.

Rand, D.A. (2008). Mapping global sensitivity of cellular network dynamics: sensitivity heat maps and a global summation law. *J.R. Soc. Interface* **5**: S59-S69.

Ruoff, P. (1992) Introducing temperature-compensation in any reaction kinetic oscillator model. *J Interdiscipl Cycle Res* **23**: 92–99.

Ruoff, P. (1994) General homeostasis in period and temperature-compensated chemical clock mutants by random selection conditions. *Naturwissenschaften* **81**: 456–459.

Ruoff, P., Vinsjevik, P.M., Rensing, L. (2000) Temperature compensation in biological oscillators: a challenge for joint experimental and theoretical analysis. *Comments Theor Biol* **5:** 361–382.

Salomé PA, Weigel D & McClung CR (2010) The role of the Arabidopsis morning loop components CCA1, LHY, PRR7, and PRR9 in temperature compensation. *Plant Cell* **22:** 3650–3661.

Zeugner, A., Byrdin, M., Bouly, J.P., Bakrim, N., Giovani, B., Brettel, K., and Ahmad, M. (2005). Light-induced electron transfer in Arabidopsis cryptochrome-1 correlates with in vivo function. *In J Biol Chem*, pp. 19437-19440.

Supplementary Figures and legends

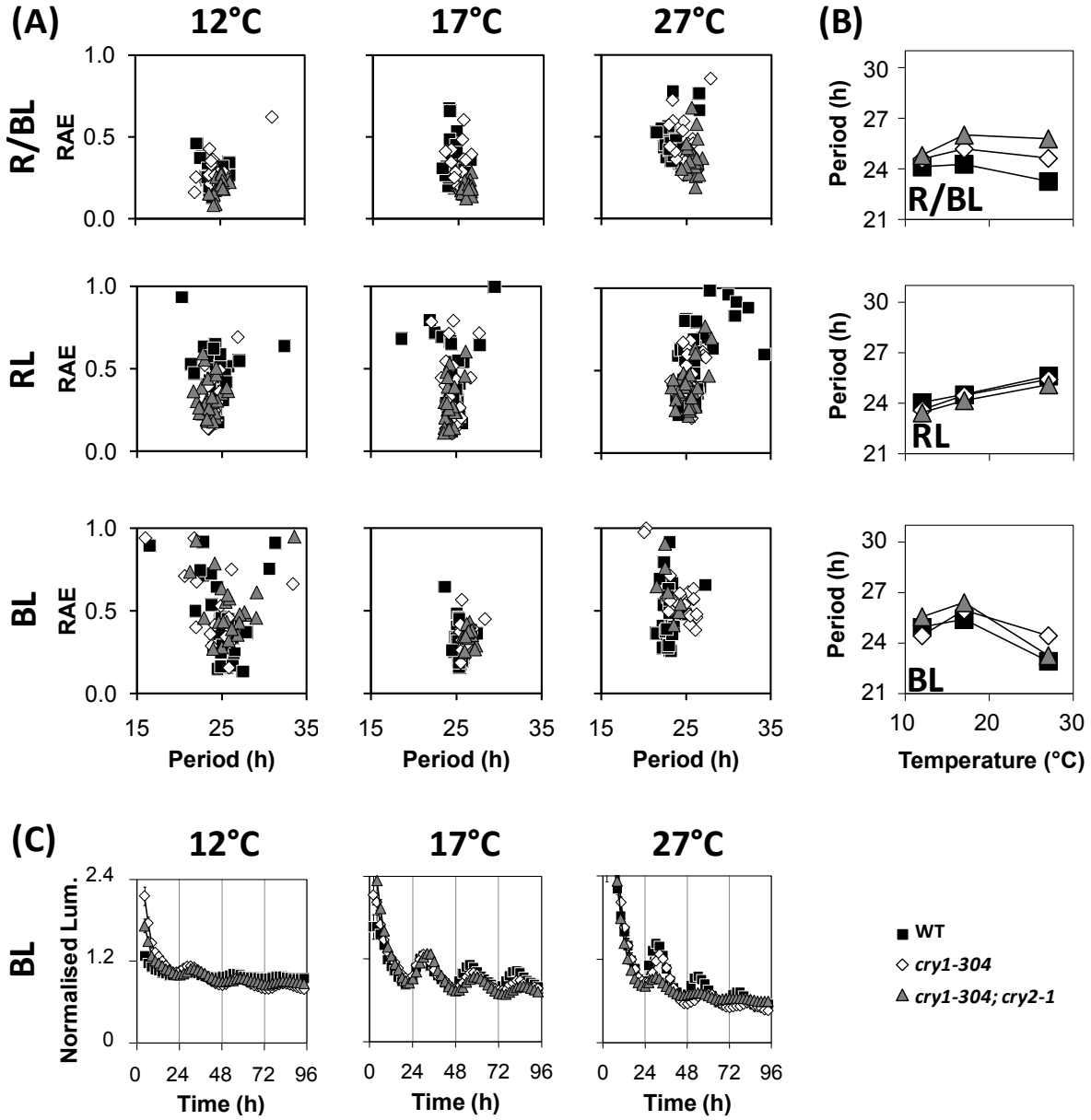

Supplementary Figure 1. The *CAB2:LUC+* reporter confirms a strong interaction of light and temperature on control of circadian period.

Transgenic Col-0 WT (black squares), *cry1* mutant (white diamonds) and *cry1 cry2* double mutant (grey triangles) seedlings expressing gene were entrained under 12L:12D cycles for 7 d, before transferring to 12°C, 17°C, or 27°C and either constant BL, RL or R/ BL. **(A)** Plots for each group of seedlings (x-axis) against Relative Amplitude Error (RAE) (y-axis), where low RAE values indicate robust rhythms. **(B)** Data shows variance-weighted mean period estimates from 4-12 groups containing three independently-transformed transgenic lines. Error bars represent variance-weighted SE. **(C)** *CAB2:LUC+* expression profiles for data from BL at 12°C, 17°C and 27°C. Each trace is normalised to the mean, error bars indicate SE. The experiment shown is representative of the three biological replicates.

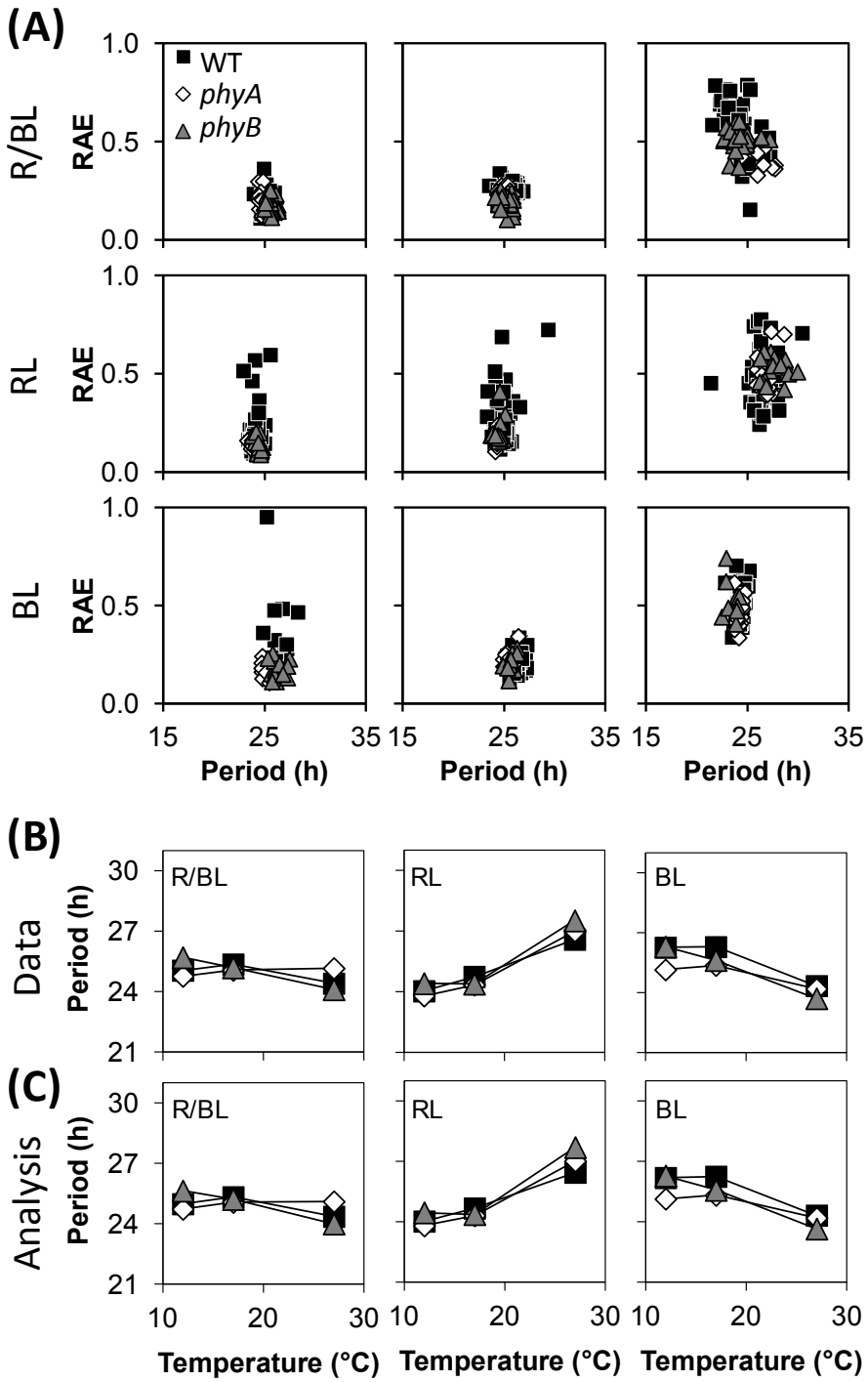

Supplementary Figure 2. The *phyA and phyB* monogenic mutation display subtle temperature dependent circadian period phenotype for the *CCR2:LUC+* marker. Transgenic Col-0 WT (black squares), *phyA* mutant (white diamonds) and *phyB* mutant (grey triangles) seedlings expressing gene were entrained under 12L:12D cycles for 7 d, before transferring to 12°C, 17°C, or 27°C and either constant BL, RL or R/ BL. **(A)** Plots for each group of seedlings (x-axis) against Relative Amplitude Error (RAE) (y-axis), where low RAE values indicate robust rhythms. **(B)** Data shows variance-weighted mean period estimates from 4-12 groups containing three independently-transformed transgenic lines. Error bars

represent variance-weighted SE. **(C).** Mean periods from only the fixed effects of the mixed-effect statistical model, which capture the variation in the data.

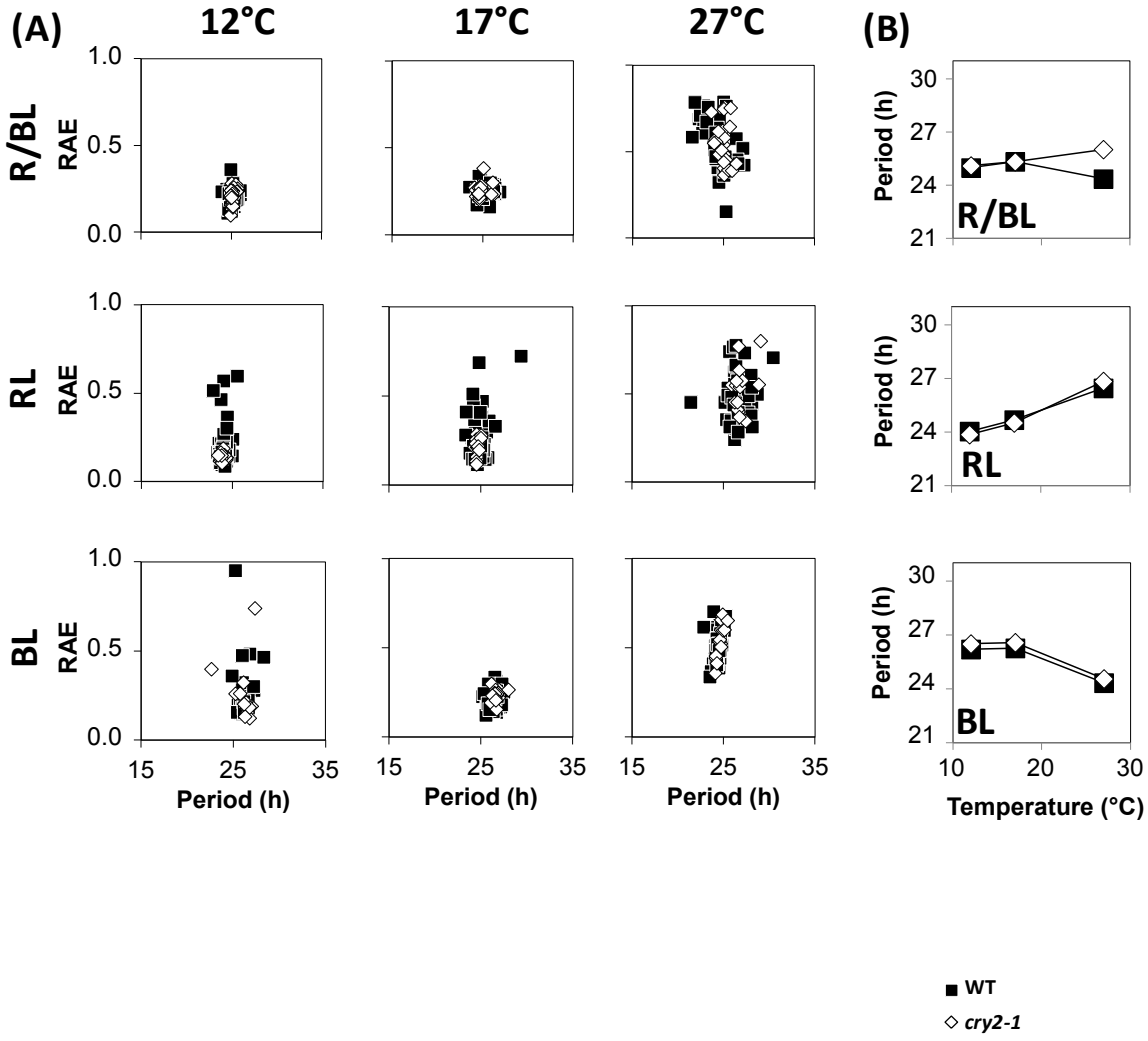

Supplementary Figure 3. The *cry2* monogenic mutation does not alter *CCR2:LUC+* circadian period.

Transgenic Col-0 WT (black squares), and *cry2-1* mutants (white diamonds) carrying the *CCR2:LUC+* reporter gene were entrained under 12L:12D cycles for 7 d, before transferring to 12°C, 17°C, or 27°C and either constant BL, RL or R/ BL. **(A)** Plot of period for each group of seedlings (x-axis) against its Relative Amplitude Error (RAE) (y-axis), where low RAE values indicate robust rhythms. **(B)** Data shows variance-weighted mean period estimates from 6-14 groups containing three independently-transformed transgenic lines. Error bars represent variance-weighted SE. The experiment shown is representative of the three biological replicates.

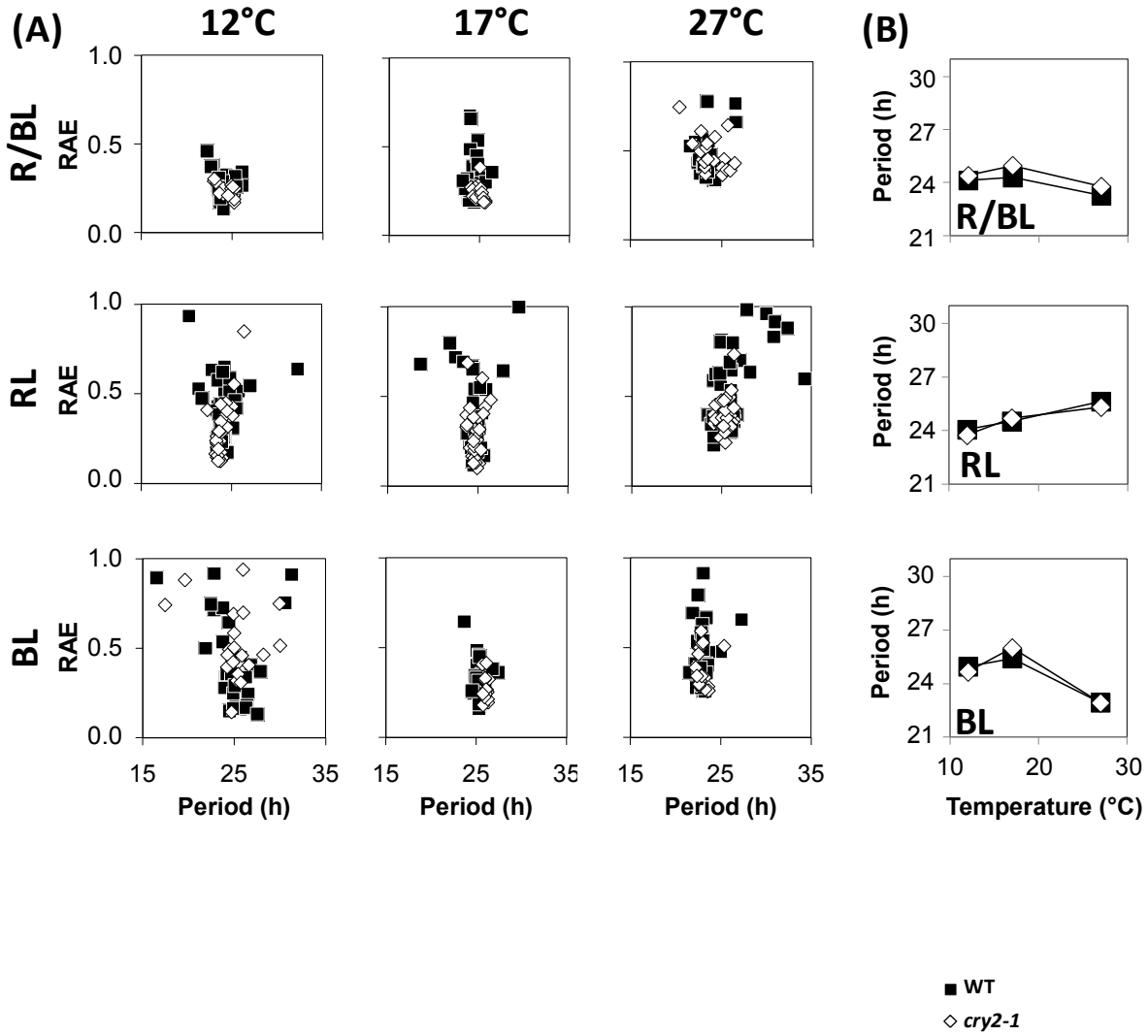

Supplementary Figure 4. The *cry2* monogenic mutation does not alter *CAB2:LUC+* circadian period.

Transgenic Col-0 WT (black squares), and *cry2* mutants (white diamonds) carrying the *CAB2:LUC+* reporter gene were entrained under 12L:12D cycles for 7 d, before transferring to 12°C, 17°C, or 27°C and either constant BL, RL or R/ BL. **(A)** Plot of period for each group of seedlings (x-axis) against its Relative Amplitude Error (RAE) (y-axis), where low RAE values indicate robust rhythms. **(B)** Data shows variance-weighted mean period estimates from 6-14 groups containing three independently-transformed transgenic lines. Error bars represent variance-weighted SE. The experiment shown is representative of the three biological replicates.

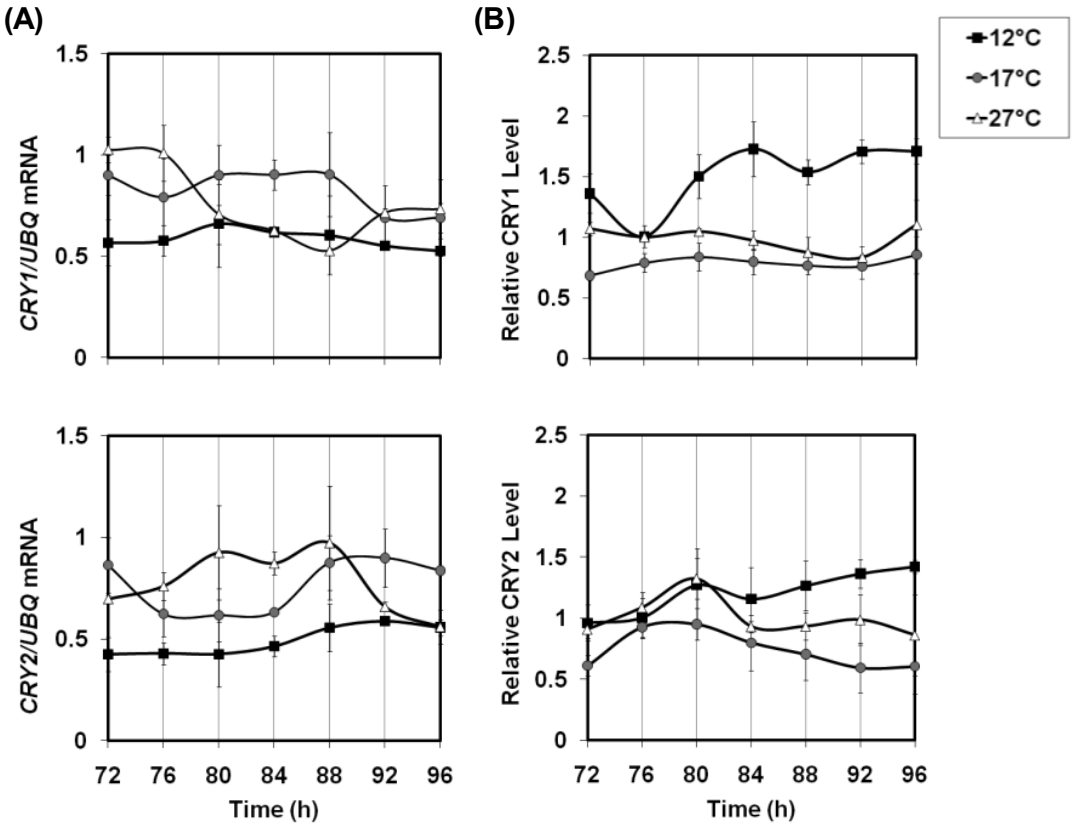

Supplementary Figure 5. Temperature effects on *CRY1* and *CRY2* expression.

WT Col-0 seedlings were entrained under 12L:12D cycles for 7 d, before transferring to constant BL at 12°C (filled squares), 17°C (grey circles) and 27°C (open triangles), and harvested every 4 h from 72-96 h after transfer.

(A) From each tissue sample, total RNA was extracted and assayed by Q-RT PCR for the accumulation of *CRY1* and *CRY2* relative to an internal *UBIQUITIN10* (*UBQ10*) control. **(B)** From each tissue sample total protein was extracted and assayed by western blotting for the accumulation of CRY1 and CRY2 protein, relative to total protein loaded. The plots represent average relative expression of CRY1 and CRY2 at 12°C, 17°C and 27°C in Col-0. Error bars indicate SE. Each data point is the average of three technical replicates. Similar results were obtained in two replicates of the same experiment; one representative experiment is shown.

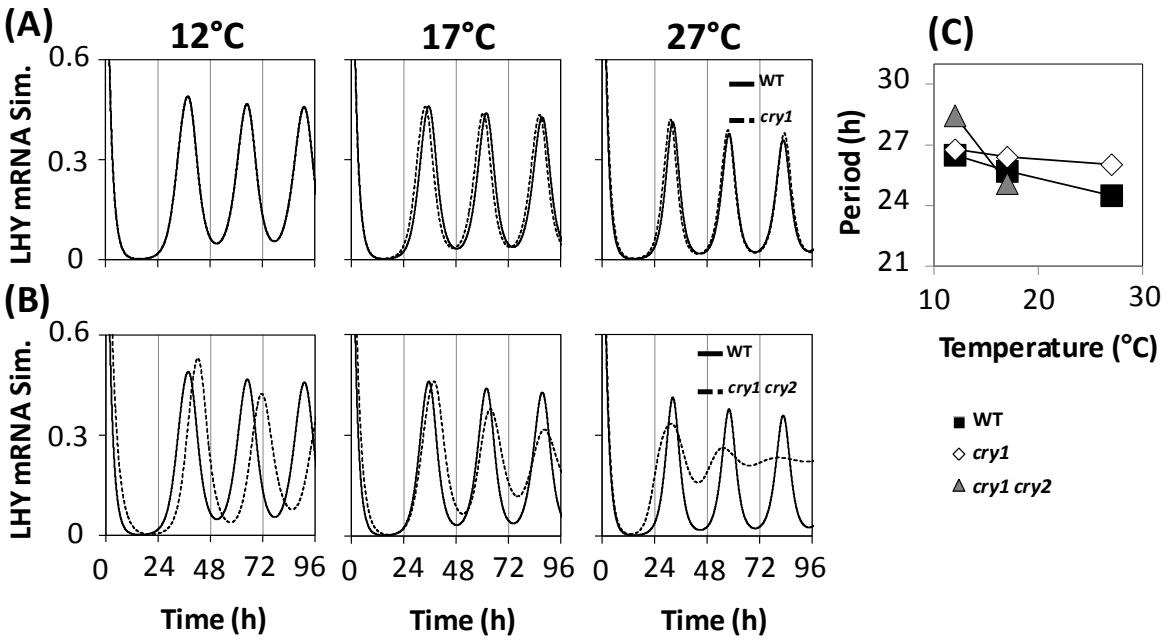

Supplementary Figure 6. Simulated behaviour of the *cry* mutants.

Simulated *LHY/CCA1* timeseries from the WT model for (A) the *cry1* single mutant at 12, 17 and 27°C (B), and *cry1 cry2* double mutant at 12, 17 and 27°C. The dashed line is the mutant and the solid line is the WT simulation. (C) shows the temperature effects on the circadian period of the model for the *cry1* and *cry1 cry2* mutant compared to WT. The open diamonds is the *cry1* mutant and the grey filled triangles is the *cry1 cry2* double mutant.

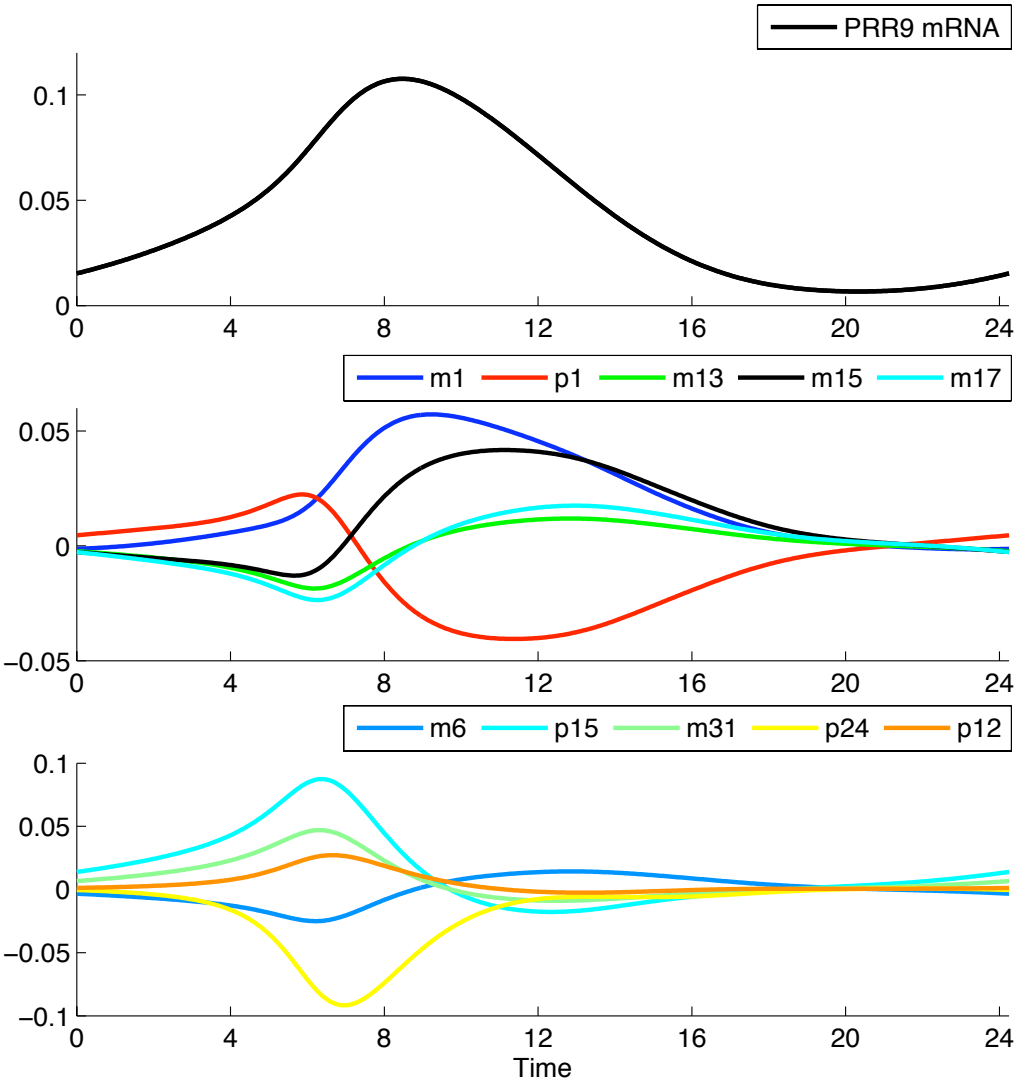

Supplementary Figure 7. (top panel) Simulated WT *PRR9* mRNA of Pokhilko et al. (2012) model over one cycle (of period 24.25h); **(middle and bottom panels)** changes to *PRR9* mRNA levels that will be incurred by changing each light parameter (morning loop parameters listed in middle panel, evening loop parameters listed in bottom panel). These changes are calculated using theory described in Rand (2008).

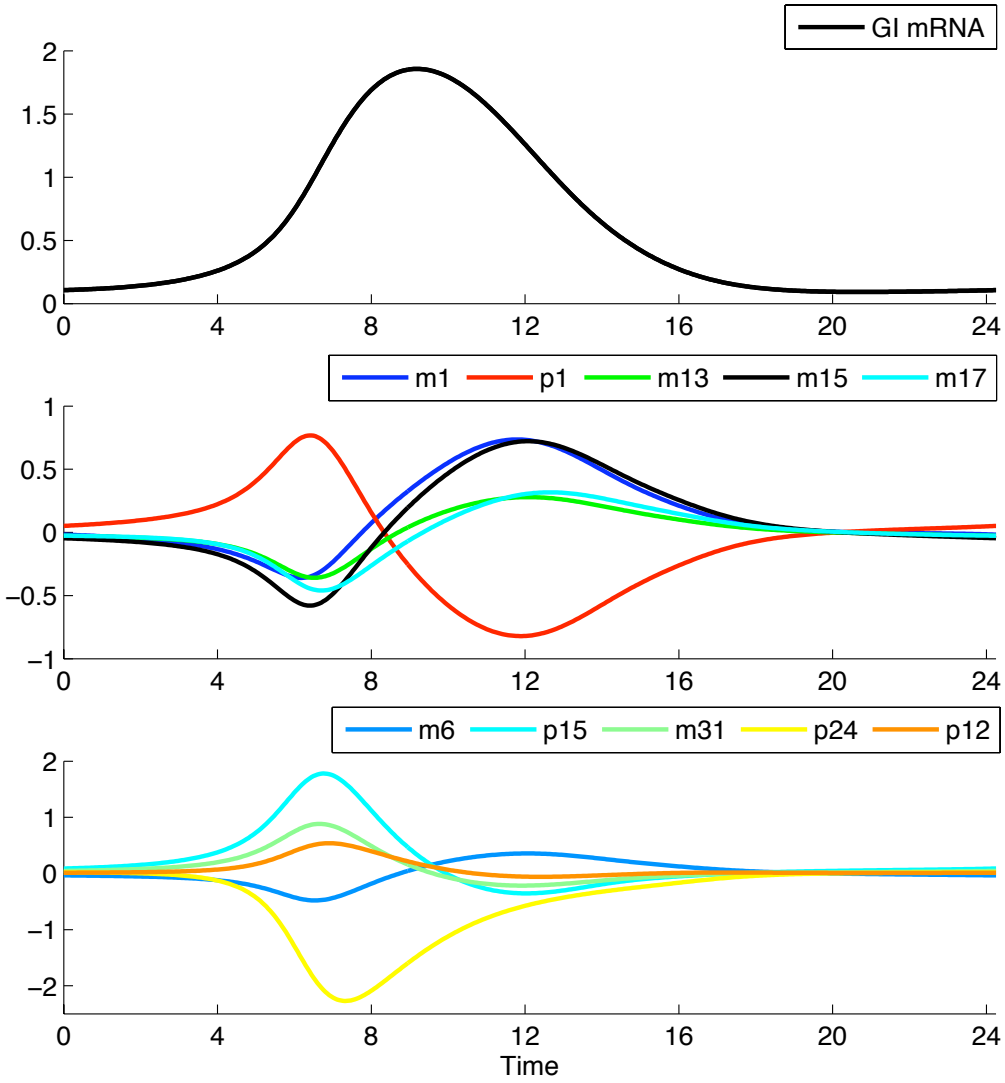

Supplementary Figure 8. (top panel) Simulated WT *GI* mRNA of Pokhilko et al. (2012) model over one cycle (of period 24.25h); **(middle and bottom panels)** changes to *GI* mRNA levels that will be incurred by changing each light parameter (morning loop parameters listed in middle panel, evening loop parameters listed in bottom panel). These changes are calculated using theory described in Rand (2008).

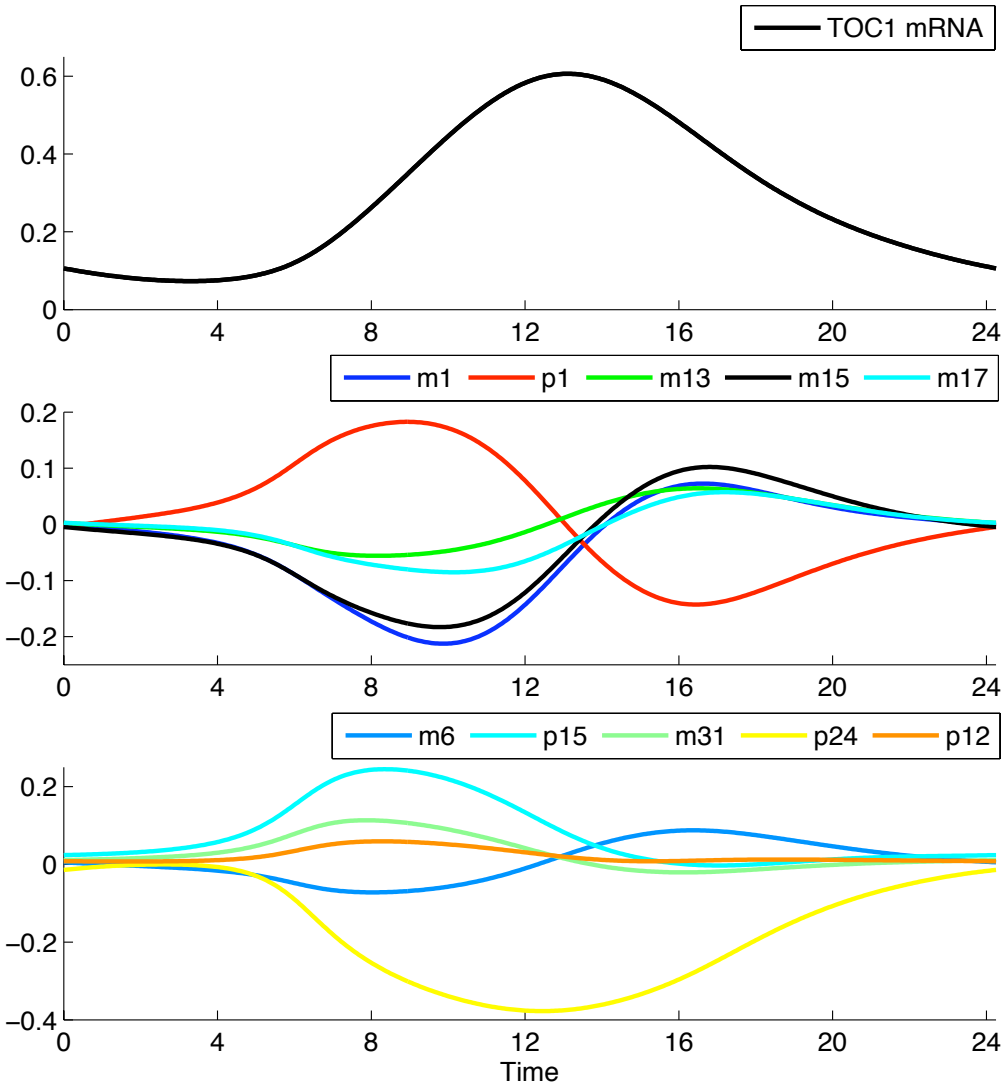

Supplementary Figure 9. (top panel) Simulated WT *TOC1* mRNA of Pokhilko et al. (2012) model over one cycle (of period 24.25h); **(middle and bottom panels)** changes to *TOC1* mRNA levels that will be incurred by changing each light parameter (morning loop parameters listed in middle panel, evening loop parameters listed in bottom panel). These changes are calculated using theory described in (Rand, 2008).

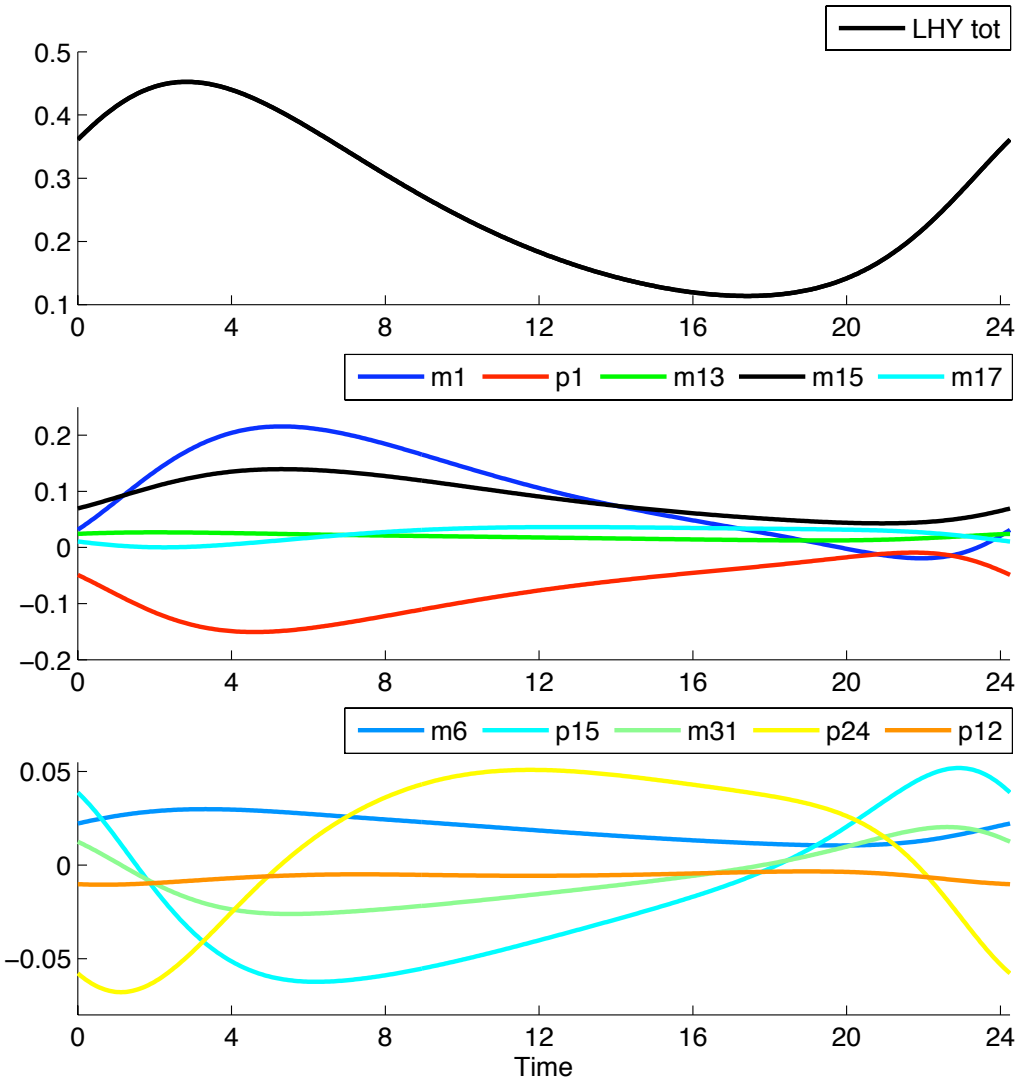

Supplementary Figure 10. (top panel) Simulated WT LHY total protein of Pokhilko et al. (2012) model over one cycle (of period 24.25h); **(middle and bottom panels)** changes to LHY total protein levels that will be incurred by changing each light parameter (morning loop parameters listed in middle panel, evening loop parameters listed in bottom panel). These changes are calculated using theory described in (Rand, 2008).

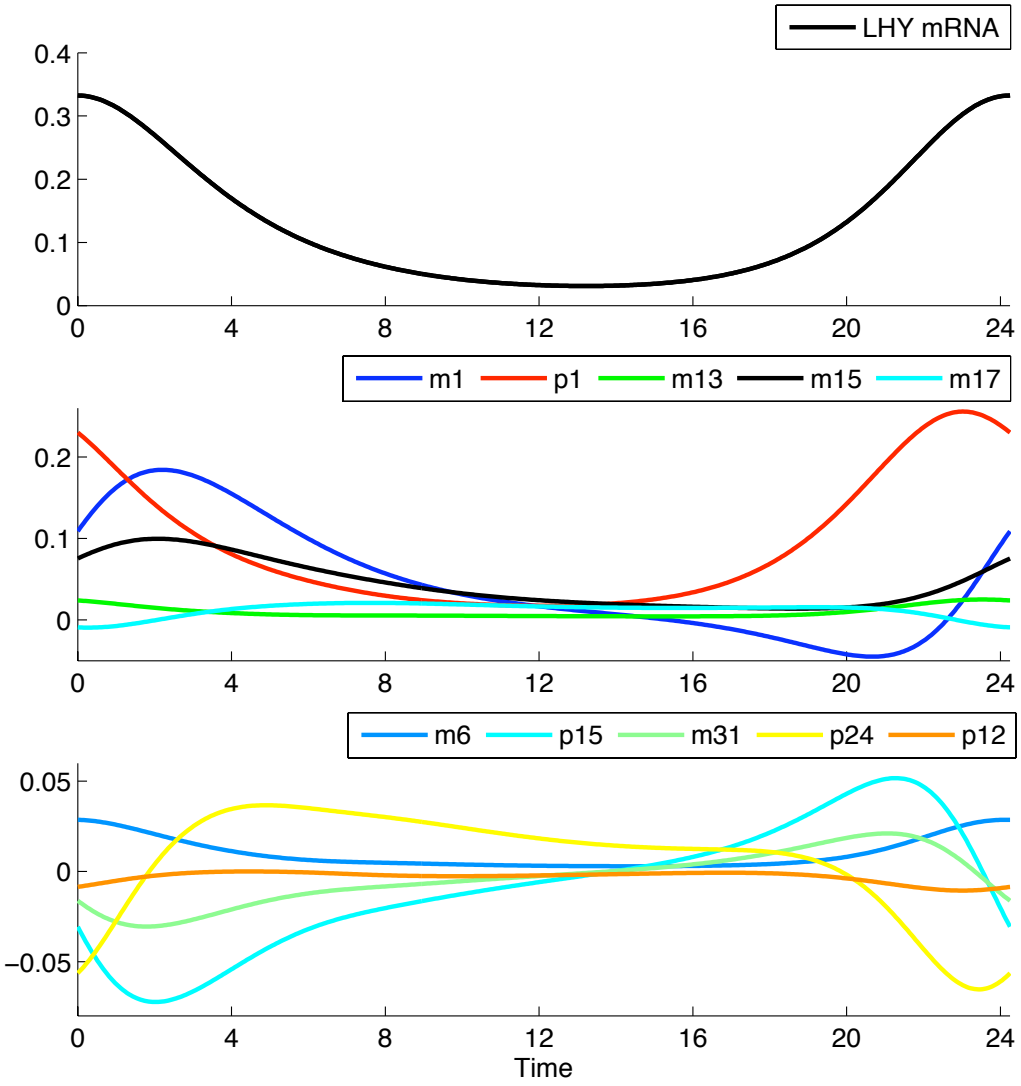

Supplementary Figure 11. (top panel) Simulated WT *LHY* mRNA of Pokhilko et al. (2012) model over one cycle (of period 24.25h); **(middle and bottom panels)** changes to *LHY* mRNA levels that will be incurred by changing each light parameter (morning loop parameters listed in middle panel, evening loop parameters listed in bottom panel). These changes are calculated described in (Rand, 2008).

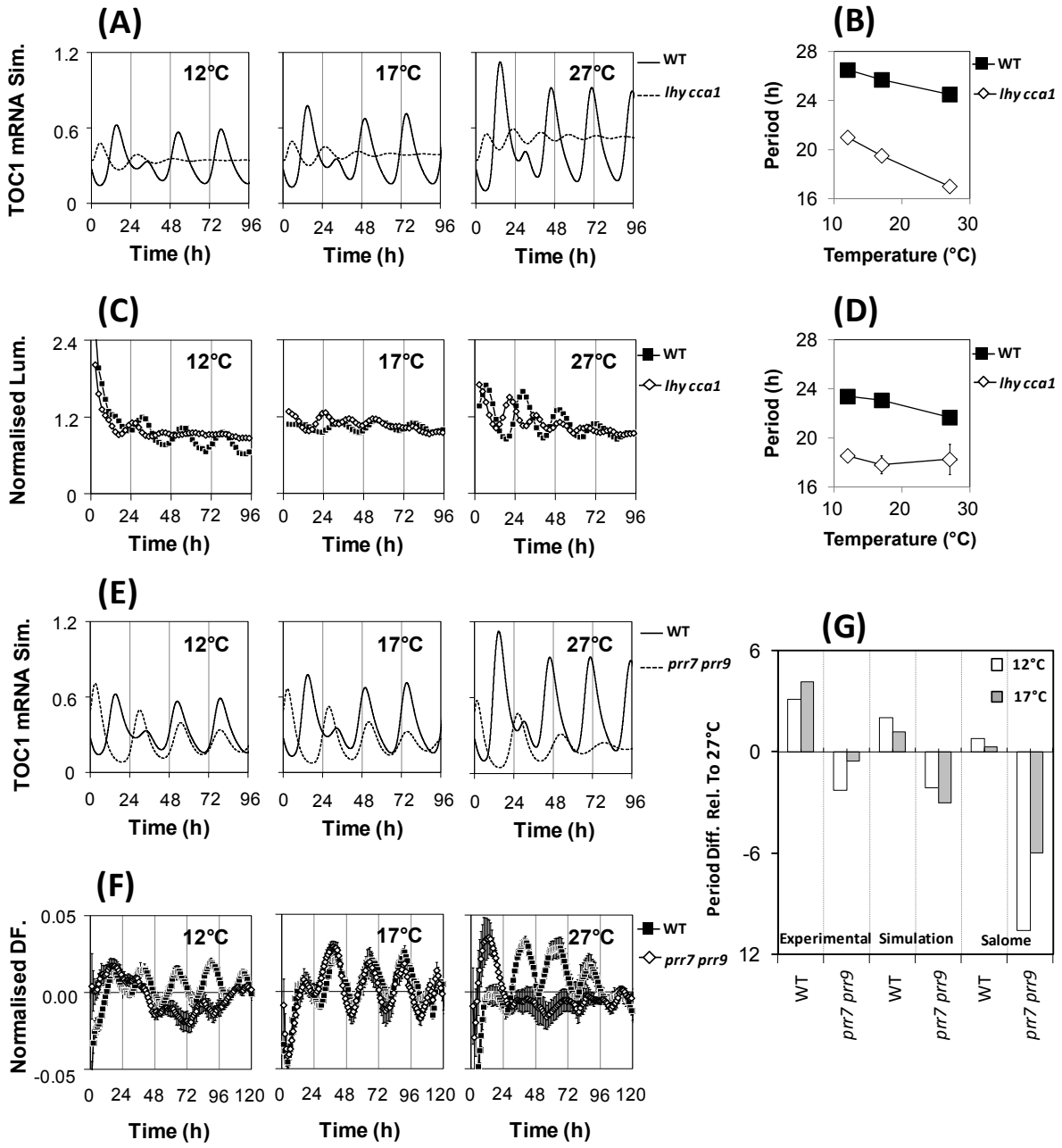

Supplementary Figure 12. Simulated behaviour of the *lhy cca1* anf the *prr7 prr9* mutants.

Simulated *TOC1* timeseries from the WT model for (A) the *lhy cca1* double mutant and (E) *prr7 prr9* double at 12, 17 and 27°C compared to WT. The dashed line represents the mutant and the solid line the WT. (B) shows the simulated temperature dependent period change of *lhy cca1* mutant versus WT. (C) *CAB2:LUC* line graph data for the *lhy cca1* double mutant at 12, 17 and 27°C. (F) Shows delayed fluorescence data for prr7 prr9 double mutant at 12, 17 and 27°C compared to WT. Delayed fluorescence is a non invasive universal assay for the circadian clock (Gould *et al*., 2009). For B, C and F the WT is the black filled squares and the mutant the empty diamonds. G shows the period difference of WT and *prr7 prr9* mutant of 12 and 17°C relative to 27°C from experimental, simulation and Salome *et al*., 2010 paper.

Factors	Estimate (hours)	Std. Error	t-Value
Intercept	24.12	0.14	175.36
BL	0.83	0.18	4.63
CCR2	0.85	0.17	5.06
27C	-0.85	0.21	-4.07
cry1cry2	0.69	0.21	3.25
cry1	0.46	0.20	2.32
phyb	0.76	0.20	3.76
RL: CCR2	-0.87	0.22	-4.03
RL:27C	2.43	0.30	8.24
BL:27C	-1.16	0.29	-3.96
RL:cry1cry2	-1.29	0.25	-5.24
RL:cry1	-0.91	0.25	-3.62
BL:cry1	-0.96	0.31	-3.13
RL:cry2	-0.58	0.27	-2.17
BL:phya	-0.62	0.27	-2.27
RL:phyb	-0.51	0.26	-1.92
17C:cry1cry2	1.05	0.30	3.48
27C:cry1cry2	1.84	0.32	5.79
27C:cry1	0.91	0.32	2.86
RL:CCR2:cry1cry2	0.92	0.36	2.56
RL:17C:cry1cry2	-0.78	0.37	-2.1
RL:27C:cry1cry2	-1.74	0.42	-4.14
BL:27C:cry1cry2	-2.13	0.53	-4.01
BL:27C:cry1	1.11	0.48	2.32
BL:17C:phyb	-0.98	0.43	-2.28
CCR2:27C:cry1cry2	1.63	0.50	3.25
CCR2:27C:cry2	1.31	0.46	2.83
CCR2:27C:phya	1.10	0.44	2.49
CCR2:17C:phyb	-1.08	0.39	-2.77
BL:CCR2:27C:cry1cry2	-1.76	0.81	-2.18
BL:CCR2:27C:cry2	-1.65	0.67	-2.47
RL:CCR2:27C:phyb	1.48	0.62	2.37

Supplementary Table 1. Results of the mixed-effect statistical model for all period data.

Significant main effects (top section) and interactions are presented, as retrieved by the function *lmer* in R. Each effect or interaction corresponds roughly to *t*-values with absolute value greater than two, indicating their significance. The largest, and most significant, effect is the period lengthening arising from the interaction of RL at 27°C.

The "Intercept" term corresponds to the mean period length of the reference condition, for the WT plants measured under R/BL at 12°C, using the *CAB2* marker. For each factor, the estimated effect (second column) can be interpreted as the additive change, in hours, in period length relative to the Intercept.

Factors	Estimate (hours)	Std. Error	p-Value
Intercept	24.09	0.11	< 2e-16
cry1cry2	-0.69	0.14	<<0.05
cry1	-0.47	0.16	<0.05
cry2	-0.34	0.16	0.03
phya	-0.34	0.15	0.02
17C	0.45	0.16	<0.05
27C	1.55	0.20	<<0.05
CCR2:27C	0.88	0.25	<<0.05
CCR2:cry1cry2	0.64	0.21	<<0.05
17C:cry2	0.50	0.23	0.03
CCR2:27C:cry1	1.15	0.40	<<0.05
CCR2:27C:phya	0.91	0.40	0.02
CCR2:17C:phyb	-0.87	0.34	0.01
CCR2:27C:phyb	1.03	0.41	0.01

Supplementary Table 2. Results from fitting the linear statistical model for data in red light only.

Significant main effects (top section) and interactions are presented together with corresponding probabilities (p-value) retrieved by the function *lm* in R. The largest effects arise from the period lengthening at 27°C, which is strongest with the *CCR2* marker and in some of the cry mutants. The "Intercept" term corresponds to the mean period length of the reference condition, for the WT plants measured at 12°C, using the *CAB2* marker. For each factor, the estimated effect (second column) can be interpreted as the additive change, in hours, in period length relative to the Intercept.

Biochemical process	Parameter (k_j) name	Arrhenius activation energy (E_j)	Parameter (k_j) value at temperature T			Period sensitivity coefficient at temp. T ($dp/dlogk_j$)		
			12°C	17°C	27°C	12°C	17°C	27°C
LHY transcription	n0	40.5939	0.1700	0.2283	0.4000	1.6373	2.0454	2.8297
LHY mRNA degradation	m1	3.6511	0.5000	0.5134	0.5400	-6.9895	-6.5706	-7.2305
LHY translation	p1	35.3172	0.1900	0.2456	0.4000	3.5077	3.2202	2.5552
TOC1 protein degradation	m6	38.9484	0.1100	0.1460	0.2500	-5.4299	-5.8425	-3.6957
TOC1mod protein degradation	m25	1.7253	0.2700	0.2734	0.2800	-6.5817	-4.8767	-0.9550
Y transcription	n5	0.0000	3.4000	3.4000	3.4000	0.5042	0.6147	0.3702
P protein degradation	m11	0.0000	1.0000	1.0000	1.0000	0.0000	0.0000	0.0000
PRR9 protein degradation	m13	0.0000	0.3200	0.3200	0.3200	0.1327	0.1210	0.1790
PRR7 protein degradation	m15	20.7914	0.2000	0.2326	0.3100	-2.1977	-1.9764	-3.9894
NI protein degradation	m17	0.0000	0.3000	0.3000	0.3000	-1.1081	-0.7156	-1.0996
GI transcription	n12	1.0203	2.3000	2.3171	2.3500	-3.0686	-3.3244	-2.1204
GI:ZTL complex formation	p12	0.0000	30.0000	30.0000	30.0000	-0.0521	-0.0562	-0.0384
					dp/dT	-0.1580	-0.0190	-0.0694
					Period (p)	26.4647	25.6808	24.5268

Supplementary Table 3. Parameter values for a temperature-compensated clock in the model of WT plants.
The parameter names in red are those that have been altered (with temperature, i.e. with non-zero E_j) to produce the temperature compensated clock thus matching experimental data. k_j are the parameter values for the three temperatures shown; are the activation energies from Arrhenius equations; $dp/dlogk_j$ are the period sensitivity coefficients; dp/dT are the ratio of d period/ d temperature; the final row shows the simulated periods.

Biochemical process	Parameter (k_j) name	*cry1 cry2* mutant Param. (k_j) value at *T*			*cry1* mutant Param. (k_j) value at *T*		
		12°C	17°C	27°C	12°C	17°C	27°C
LHY transcription	n0	0.1400	0.1497	0.1700	0.1700	0.2283	0.4000
LHY mRNA degradation	m1	0.3300	0.3911	0.5400	0.5000	0.5134	0.5400
LHY translation	p1	0.1900	0.1900	0.1900	0.1900	0.2456	0.4000
TOC1 protein degradation	m6	0.2000	0.2705	0.4800	0.1100	0.1460	0.2500
TOC1mod protein degradation	m25	0.2700	0.2734	0.2800	0.2700	0.2734	0.2800
Y transcription	n5	1.8000	1.8666	2.0000	3.4000	3.4000	3.4000
P protein degradation	m11	1.0000	1.0000	1.0000	1.0000	1.0000	1.0000
PRR9 protein degradation	m13	0.3200	0.5451	1.5000	0.3200	0.5451	1.5000
PRR7 protein degradation	m15	0.2000	0.2326	0.3100	0.2000	0.2326	0.3100
NI protein degradation	m17	0.3000	0.3284	0.3900	0.3000	0.3000	0.3000
GI transcription	n12	1.8000	1.8339	1.9000	2.3000	2.3171	2.3500
GI:ZTL complex formation	p12	30.0000	30.0000	30.0000	30.0000	30.0000	30.0000
	Period (*p*)	28.3550	25.08333	AR	26.8733	26.1033	25.8700

Supplementary Table 4. The parameter sets for the models of the *cry1 cry2* double mutant and *cry1* single mutant, across the temperature range from 12° to 27°C. Parameter names in red were altered compared to WT in one or both mutants. The simulated period phenotypes of the mutants are shown in the bottom row and are for *LHY* mRNA simulations.

At	Gene Name	Forward	Reverse	Source
At2g46830	CCA1	GATGATGTTGAGGCGGATG	TGGTGTTAACTGAGCTGTGAAG	Hall et al., 2003
At4g08920	CRY1	GCAGAATCACCATGAAATACTG	CAGCCCTTATGATGTTCCTC	-
At1g04400	CRY2	AGAGACATGAAGAAATCTAGGG	TGAATACCTTCCAGATTCTTCC	-
At1g22770	GI	GGTCGACGGTTTCTCCAATCTA	CGGACTATTCATTCCGTTCTTC	Hall et al., 2003
At1g01060	LHY	CAACAGCAACAACAATGCAACTAC	AGAGAGCCTGAAACGCTATACGA	Edwards et al., 2006
At5g02810	PRR7	CTTTCTCAAGGTATAATCCAGCC	ACAATCATATGCTGCTTCAGTC	-
At2g46790	PRR9	GATTGGTGGAATTGACAAGC	TCCTCAAATCTTGAGAAGGC	-
At5g02810	TOC1	ATCTTCGCAGAATCCCTGTGATA	GCACCTAGCTTCAAGCACTTTACA	Edwards et al., 2006
At4g05320	UBQ10	CACACTCCACTTGGTCTTGCGT	TGGTCTTTCCGGTGAGAGAGTCTT	Czechowski et al., 2004

Supplemental Table 5. Primers used for QT-PCR.

Table contains At number, gene name, forward/ reverse primers and the source of the primers. Any primers which have no source were created in house using Perlprimer (http://perlprimer.sourceforge.net) (Marshall, 2004).

Biochemical process	**Parameter (k_j) name**	**Parameter (k_j) value at temperature T** 27°C		**Period sensitivity coefficient at temp. T ($dp/dlogk_j$)** 27°C
LHY mRNA degradation	m1	0.54		-3.18
LHY translation	p1	0.40		0.31
TOC1 protein degradation	m6	0.3		-0.99
P protein degradation	m11	1.00		0.00
PRR9 protein degradation	m13	0.32		-0.76
PRR7 protein degradation	m15	0.70		-0.52
NI protein degradation	m17	0.50		-0.97
GI:ZTL complex formation	p12	3.40		-0.22
COP1 cytoplasmic and night form degradation	p15	0.40		-0.23
COP1 day form degradation	m31	0.30		0.17
EC complex protein degradation	p24	2.00		2.60
			Period (p)	24.25

Supplementary Table 6. Light parameter values for the Pokhilko et al. (2012) model.

The parameter names in red are those that did not exist in the Pokhilko et al. (2010) model. *kj* are the parameter and *dp/dlogkj* are the period sensitivity coefficients; dp/dT are the ratio of d period/ d temperature; the final row shows the simulated periods. Note that parameters have been modified from the Pokhilko et al, (2012) to perform the analysis. Original rates with day and night parameter values have been rewritten in the form (k1*L+k2*(1-L)) where k1 and k2 indicate values when lights are 'on' and 'off' respectively. LHY translation is changed from (p2+p1*L) to (p1*L+p2*(1-L)),and p1 value is changed from 0.13 to 0.4. Protein degradations of TOC1, PRR9, PRR7 and NI protein originally occur in the model as (k1+k2*(1-L)) and here they are modified to take the form (k1*L +k2*(1-L)). TOC1 degradation is rewritten as (m6*L+m7*(1-L)) and value of m7 is changed to 0.7. Similarly for PRR9, PRR7 and NI degradation parameters, values of m22 (changes from 0.1 to 0.42) , m23 (1.8 to 2.5) , m24 (0.1 to 0.6). COP1 day active form degradation of type m31*(1+m33*(1-L)) has been rewritten as

(m31*L+m33*(1-L)) so m33 is changed from 3.9 to 4.2, COP1 night and cytoplasmic protein degradation has the parameter m27*(1+p15*L) and this is now rewritten as (m27*(1-L)+p15*L) and p15 value is changed from 0.3 to 0.4. EC light degradation was originally written as m32*p24*L and here it is rewritten as p24*L with p24 value changed from 10 to 2.

Light	Temperature	Repeat	Biodare Code
BL	12°C	1	13390646057710
BL	12°C	2	13390720965302
BL	12°C	3	13390757095644
BL	17°C	1	13390700146009
BL	17°C	2	13390716217061
BL	17°C	3	13390766559885
BL	27°C	1	13390707022980
BL	27°C	2	13390726557783
BL	27°C	3	13390776176796
RBL	12°C	1	13391556580623
RBL	12°C	2	13391584568887
RBL	12°C	3	13391620137471
RBL	17°C	1	13391579462696
RBL	17°C	2	13391596408158
RBL	17°C	3	13391620325732
RBL	27°C	1	13391550627332
RBL	27°C	2	13391602100179
RBL	27°C	3	13391620428613
RL	12°C	1	13390801847617
RL	12°C	2	13390805417188
RL	12°C	3	13390844096246
RL	12°C	4	13390844168307
RL	17°C	1	13390818841409
RL	17°C	2	13390824812831
RL	17°C	3	13390844299928
RL	17°C	4	13390844394269
RL	27°C	1	13390841628455
RL	27°C	2	13390832805592
RL	27°C	3	13390844487550
RL	27°C	4	13390844590371

Supplementary Table 7. Codes for accessing all experiments analysed in this paper. From Biodare (www.biodare.ed.ac.uk) all raw data can be accessed and downloaded in excel format.